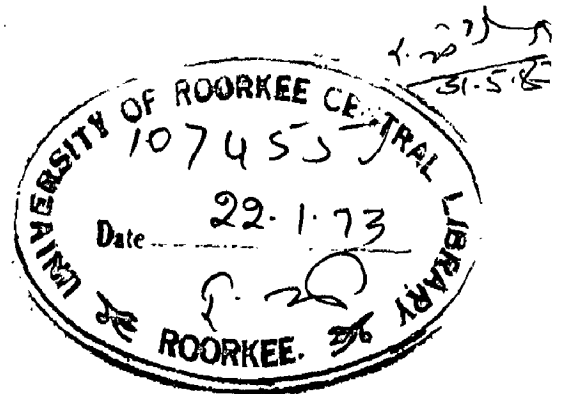


# AIR ENTRAINMENT IN FLOWS ON STEEP SLOPES

A DISSERTATION  
submitted in partial fulfilment of the  
requirements for the award of the degree  
of  
MASTER OF ENGINEERING  
in  
WATER RESOURCES DEVELOPMENT

By  
**H. K. GARG**

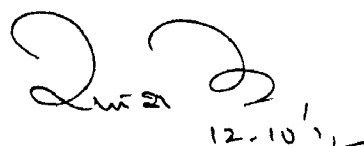


WATER RESOURCES DEVELOPMENT TRAINING CENTRE  
UNIVERSITY OF ROORKEE  
ROORKEE (INDIA)  
October, 1972

CERTIFICATE

Certified that the dissertation entitled, "AIR ENTRAINMENT IN FLOWS ON STEEP SLOPES" which is being submitted by Sri H.K. Garg in partial fulfilment of the requirements for the degree of MASTER OF ENGINEERING in Water Resources Development of University of Roorkee, is a record of student's own work carried out by him under my supervision and guidance. The matter embodied in this has not been submitted for any other Degree or Diploma.

This is further to certify that he has worked for a period of nine months from January 1972 to October 1972 in connection with the preparation of this dissertation.



12.10.72

(R.S. VARSHNEY)  
Executive Engineer (Yamuna Project)  
Formerly Reader on deputation at  
Water Resources Development Training  
Centre, University of Roorkee,  
Roorkee.

## ACKNOWLEDGEMENTS

Deep sense of gratitude is expressed for the unremitting encouragement and help given from time to time by Dr.R.S. Varshney, Executive Engineer, Yamuna Project, Dehradun formerly Reader on deputation at Water Resources Development Training Centre, Roorkee. Without his able guidance this humble piece of work could never come up.

The active help given by Smt. Meera Garg, wife of the author, can not be forgotten. She gladly accepted trials and tribulations while the author burnt midnight oil.

Thanks are due to Sri A.S. Chawla, Research Officer and Sri N.L. Gaur, Assistant Research Officer, Irrigation Research Institute, Roorkee for their help in making several of the references available for study.

The author is also grateful to Sri N.K.Agrawal, Superintending Engineer, Tehri Bandh Pariyojna Mandal, Roorkee for his kind permission to work for this dissertation.

H.K. GARG

## SYNOPSIS

Entrainment of air in high velocity open channel flow causes bulking of flow and alters normal frictional resistance and other flow properties. Thus design problems of proper free board allowance and calculation of modified channel dimensions arise.

An attempt has been made to compile the studies done in the field and hydraulic laboratories by various investigators. Based on these studies a suitable design procedure for air entrained flow has been evolved and conclusions have been drawn regarding the various aspects of air entrainment phenomenon in open channel flow. The presentation will be useful to the design engineers whose interest in the subject is growing fast with more and more high head structures coming up.

## CONTENTS

CHAPTER	PAGE
CERTIFICATE	
ACKNOWLEDGEMENTS	
SYNOPSIS	
CONTENTS	
1. INTRODUCTION	
1.0 The Phenomenon of Air Entrainment	1
1.1 Importance of Air Entrainment in Field	1
1.2 Types of Air Entrainment	2
1.3 Brief Review of Work Done	4
1.4 Scope of Dissertation	6
2. REVIEW OF FIELD STUDIES	
2.0 Introduction	8
2.1 Prototype Observations on Spillway Faces	8
2.2 Studies on Natural Chutes in U.S.A.	10
2.3 Studies on Natural Chutes in Yugoslavia	16
3. REVIEW OF LABORATORY STUDIES	
3.0 Introduction	20
3.1 Studies in the Neyrpic Laboratory, France	20
3.2 Studies in the Laboratory of University of Naples, Italy	23
3.3 Studies at the St. Anthony Falls Labora- tory, U.S.A.	30
3.4 Studies at the Central Water and Power Research Station, Poona	40
3.5 Studies at Indian Institute of Science, Pangalore	42
4. DESIGN PROCEDURE	
4.0 Introduction	54
4.1 Commencement of Air Entrainment	54

## CONTENTS (Contd.)

CHAPTER	PAGE
4.2 Mean Air Concentration	55
4.3 Bulkage Depth and Height of Guide Walls	56
5. CONCLUSIONS	
5.0 Introduction	59
5.1 Mechanism of the Phenomenon	59
5.2 Inception of Air Entrainment	60
5.3 Distribution of Velocity in Aerated Flow	61
5.4 Distribution of Air Concentration	61
5.5 Factors Affecting Air Entrainment	62
5.6 Effects of Entrained Air on the Flow	64
APPENDIX	
I REFERENCES	67
II NOTATION	70
III FIGURES	73

## CHAPTER - 1

### INTRODUCTION

#### 1.0 THE PHENOMENON OF AIR ENTRAINMENT

Air entrainment is a surface phenomenon in which atmospheric air is insufflated into and mixed with the flow to create the appearance of "white water" with its violently agitated and ill-defined free surface. This condition is frequently observed in flows down steep chutes and spillways. Air entrainment is actually a continuous process of droplets of water projecting from the liquid into the air above and air bubbles penetrating into the liquid mass. It occurs when the transverse velocities of turbulence are sufficiently strong near the air-water interface to cause clumps of water to break through the surface into the air and then fall back by gravity into the flowing stream. While projecting up and then falling back these clumps of water break into a heterogeneous spray of globules and droplets which engulf a certain amount of air leading to insufflation of air into the stream. The air carried back is then distributed throughout the flow by turbulent transfer. As the relative densities for air and water are about 1:800, there is a strong tendency for the air to get separated from the flowing water. Against this tendency acts the turbulence of flow which carries the air downward.

#### 1.1 IMPORTANCE OF AIR ENTRAINMENT IN FIELD

In classical hydraulics the presence of another ambient fluid such as air is not taken into consideration while studying the flow of water. However a great number of hydrodynamic phenomena are affected by air entrainment; the water depths may increase greatly, there may be an appreciable effect on friction loss, mean flow velocity, etc. The phenomenon as such may no longer be

neglected. In the absence of the knowledge of air entrainment laws it has been a practice to provide a liberal arbitrary allowance for air bulking in the design of free boards for training walls and hydraulic jump aprons at the toes of spillways. The phenomenon of air entrainment therefore assumes great importance, hydraulic and economic, for the ~~designing~~ <sup>design</sup> hydraulic engineers. The important practical cases of air entrainment include flow down spillway faces of high dams, steep chutes, training walls, hydraulic jump aprons and energy dissipation at the toes of dams.

## 1.2 TYPES OF AIR ENTRAINMENT

The phenomenon of air entrainment in water flowing in a channel or discharging freely into the atmosphere may be sporadic or general as regards surface area occupied, superficial or complete in respect to depth affected and intermittent or continuous with regard to progression or frequency of occurrence. The observed air entrained flows have been broadly classified as below by Michels and Lovely<sup>22</sup>,

1. Rippled Flow - This presents generally a smooth surface undulation and no air entrainment as in a gently sloping uniform channel or in upper reaches of a steep chute. The velocity is low or medium and turbulence is small.

2. Choppy Flow - The surface is generally agitated with only a small proportion occupied at any instant by individually breaking or mutually interfering waves which, sporadically and intermittently envelope air and release it soon after subsiding. Practically no sensible increase in flow depths occurs. Examples are the flow in a gently sloping natural stream having an irregular bed or in a uniform channel of medium slope or near obstructions



in an otherwise gently sloping invert. The flow is characterized by larger surface variations, greater local turbulences and upward velocity components and local increases in energy gradients.

3. Scarified Flow - An air water mixture is formed generally as a relatively thin layer at the surface of a stream. The air is trapped by water particles upon their leaving the surface and small or moderate increase in flow depths occur<sup>s</sup>. Examples are the flow down rapids having an approximately uniform and gentle grade but with moderately uneven bed, or long uniform chutes of narrow widths and/or with uneven wall surfaces. It is characterized by large variations in water surface and considerable upward velocity components, generally greater velocities and energy gradients throughout the length of flow.

4. Emulsified Flow - This represents the most important air entrained open channel flow with a general, deep and continuous emulsification of air and water presenting a frothy uneven surface. The flow depths may greatly exceed those computed without allowing for air entrainment. Examples are flow down a steep wide chute or spillway surface, flow over rapids with steep and uneven bed. In such flows turbulence level is considerably high.

5. Ebullient Flow - There is a violent air-water mixture occurring<sup>n</sup> as a 'boil' on the surface, extending irregularly through a portion of the water. The air is drawn in at the free surface of the turbulent impact zone existing between a rapidly moving stream and a slack or slowly moving body of water. The air thus entrained may be recirculated in a vertical roller but generally it escapes gradually in the direction of reduction of turbulence. The depth of flow is locally increased but diminishes as turbulence is

damped out and air escapes. Examples are flow of a high velocity jet, laterally at the bed or surface level, or vertically upwards or downwards into an energy dissipator or a natural pool. It is characterized by large vertical components of velocity and high local energy gradients and generally small lateral velocities beyond zone of impact.

6. Spraying Flow - The flow is in the form of a spray such as of a jet from a needle outlet discharging into air. With sufficient velocity and distance of travel the jet breaks up into a spraying flow which finally consists of fine droplets or mist containing enmeshed air.

7. Separation Flow - High velocity flow in an open waterway and separation from a solid boundary causes reduction and instability of pressure. If the local pressure becomes subatmospheric considerable air and vapour volumes are produced. Tremendous local boundary turbulence occurs accompanied by entrainment from the atmosphere at any adjacent free surface with considerable local increase in depth of water. The flow past a gate slot in the pier and high velocity flow around baffle blocks on the floor of the energy dissipator may be quoted as examples.

### 1.3 BRIEF REVIEW OF WORK DONE

Interest in a thorough investigation of the laws of air entrainment has been aroused only in the past few decades because of more and more high head structures coming up. In the case of spillway faces one of the first studies <sup>was that</sup> ~~were these~~ by G.H.Hickox<sup>16</sup> (1945). The data indicate a functional relationship between the distance from the crest to the start of air entrainment and the unit discharge. Some work on spillway models was also reported

by Pavel<sup>23</sup> (1951). Further investigations were reported by Michels and Lovely<sup>22</sup> (1953) on Glenmaggie dam and Werribee diversion weir.

The pioneering work on air entrained flows in open channels is due to Ehrenberger<sup>12</sup> (1926) who loosely divided the flow into several zones: water near the flume floor, individual air bubbles in water, mixture of air and water, individual drops of water in air and an overlying movement of air. He also devised a simple yet effective Pitot tube to measure the air concentrations, which was first such apparatus used.

The first extensive series of observations on air entrained flow were taken by L. Standish Hall<sup>15</sup> (1943) in some hill chutes. Studies were made of air-bulking, effects on mean velocities and effects of curvatures of channels and an effort was made to correlate the air concentration with the local Froude number. Lane<sup>20</sup> (1936) has carried out similar studies on steep chutes. One of his important conclusions, which is borne out by later measurements, is that the turbulence caused by the boundary layer development extends throughout the region of flow in the case of a fully air-entrained flow. Pavel's<sup>23</sup> (1951) observations have indicated that the channel slope should exceed a certain minimum value for air entrainment to occur. Field studies on two Yugoslavian flumes have been reported by Jevdjevich and Levin<sup>18</sup> (1953)

Air entrainment studies on specially constructed laboratory flumes have been carried out at various places. Observations on a 1:1 slope and other two flatter slopes with smooth concrete walls are reported by Viparelli<sup>33, 34</sup> (1953, 57).

Detailed and exhaustive observations in a specially constructed laboratory flume have been reported by St. Anthony

Falls Laboratory<sup>1,30,31</sup> in the United States for a considerable range of discharges and at all flume slopes from vertical to horizontal. The experiments have revealed that customary open channel flow relationships do not apply to air-entrained flows. The actual velocities are shown to be higher than computed velocities by hitherto proposed methods. Special electronic apparatus, using a pair of electrodes, as probes was developed for measurement of air concentrations.

Air concentration and velocity distribution for aerated flows have also been reported by the Neyrpic Laboratory<sup>14</sup>, France, where the observations were taken in a specially designed tilting flume.

In India considerable work on different flume slopes and discharges is reported by Central Water and Power Research Station, Poona (1952-59). Tests were made in a 0.9 m wide flume and have included observations on velocity traverses, water surface profiles, distribution of air concentration and their relationship with local Froude numbers.

The Indian Institute of Science, Bangalore, have carried out extensive laboratory studies on the inception of air entrainment in steep chutes and the characteristics of self-aerated flows. The work has been reported by Rao, Gangadhariah and Seetharamiah<sup>24,25,26</sup> (1970,71).

#### 1.4 SCOPE OF DISSERTATION

The problem of air entrainment in flows on chutes and spillways is very important as design of floor and side walls is dependent on correct evaluation of depth of flow and its density.

The work done in various laboratories and field alongwith their theoretical background has been compiled and design procedure

has been formulated. The analysis presented will be helpful to design engineers engaged in designing spillways and chute channels.

## CHAPTER - 2

### REVIEW OF FIELD STUDIES

#### 2.0 INTRODUCTION

Interest in the study of the phenomenon of air entrainment made various investigators and questers to find some correlation between the flow and air entrained. Unfortunately the phenomenon in models is not governed by the Froudian relationship to the prototype observations. With a view to design high head hydraulic structures, it was therefore necessary to make detailed studies in the field to quantify the air insufflation and its effects. The work done in the field is described in this chapter.

#### 2.1 PROTOTYPE OBSERVATIONS ON SPILLWAY FACES

G.H. Hickox<sup>16</sup> made observations on spillway flow on Norris dam and on Douglas dam of T.V.A. in connection with a study of aerated flows. He concluded that in the case of water flowing down a spillway face, the distance from the crest at which air entrainment begins, increases as the unit discharge over the crest increases.

Further observations and measurements were made on spillway of Glenmaggie dam and Werribee diversion weir by Michels and Lovely<sup>22</sup>. The profiles of these are shown in fig.1. The Glenmaggie dam is a concrete gravity structure with a 113 m long spillway section which is 15 m high from apron to ogee crest. Training walls are 1.5 m high and piers 1.1 m thick are spaced at 8.5 m along the crest. Observations were made of the point of commencement of air entrainment. Discharge was calculated by conventional methods, also the velocity values and therefrom the depths of flow were computed for various discharges at the point of commencement of air entrainment. On the Werribee diversion weir which is a

3.7 m high concrete overfall weir, similar observations were taken and computations done. The results are plotted in the form of curves of  $L/d$  v.s.  $q$  (Fig.3) and  $q$  v.s.  $L$  (Fig.4), where  $L$  = distance from the leading edge of upstream curve to point of commencement of air entrainment,  $d$  = depth of flow at the same point and  $q$  = discharge per metre width of crest. These results together with visual observations indicated that complete and continuous air entrained flow commences only at a distance below the crest which increases with the discharge. The increase in this length, with increased discharge and correspondingly with increased depth of flow together with the visual observations of beginning of characteristic roughening of water surface just before the water turns white, suggests the possibility that surface entrainment of air begins at the point where the turbulence generated at the concrete-water interface reaches the surface or in other words when the thickness of the turbulent boundary layer coincides with the depth of flow.

This is also brought out by a tentative application of the boundary layer theory. The thickness of turbulent boundary layer along a flat plate under the ideal conditions of zero pressure gradient and constant undisturbed velocity is given by

$$\delta = 0.377 \left( \frac{\nu}{V} \right)^{0.2} L^{0.8} \dots\dots (1)$$

Where  $\delta$  = Thickness of turbulent boundary layer (metre)

$L$  = Distance from the leading edge (metre)

$\nu$  = Kinematic viscosity ( $m^2/sec$ )

$V$  = Undisturbed velocity at the section ( $m/sec$ )

Assuming a similar expression for the thickness of turbulent boundary layer along the flat portion of spillway,

$$\delta = K L^{\frac{1}{m+1}} \left( \frac{\nu}{V} \right)^{\frac{m}{m+1}} \dots (2)$$

Putting  $V = \frac{q}{\delta}$ , and taking kinematic viscosity of water  $\nu = 1.12 \times 10^{-6} \text{ m}^2/\text{sec}$ , it is found that the above equation agrees closely with the curve of  $\frac{L}{\delta}$  v.s.  $q$  if  $\wedge$  giving at the point of commencement of air entrainment, we choose (arbitrarily)  $m = -\frac{1}{12}$  and  $K = \frac{1}{700}$

$$\delta = \frac{L q^{1/12}}{130} \dots (3)$$

Michels and Lovely suggest the use of this formula to compute the point of commencement of air entrainment for such spillways.

## 2.2 STUDIES ON NATURAL CHUTES IN U.S.A.

L. Standish Hall<sup>15</sup> has done extensive work on three natural chutes in the U.S.A., Hat Creek No.2, Rapid flume, and the South canal chute. The distances were measured along the actual slope of the chutes, stations being marked every 7.5 m or 15 m. The discharge measurements were made in the power canals above the chutes, using Price and Hoff current meters. Velocity measurements between various stations along the chutes were made by using a colouring matter, Fluorescein or Potassiumpermanganate. A brief general description of the three chutes is given below:

Name of chute	Hat creek chute	Rapid flume	South canal chute
Surface	concrete	wooden	concrete
Length	124.6 m	204 m	1075 m
Vertical drop	57.6 m	44.2 m	42.6 m
Width	1.75 m	1.4 m	2.14 m

There are a number of changes in bed slope and vertical and horizontal curves in the alignment of all the three chutes. The



profiles of the Hat creek and Rapid flume are shown in figs.5 and 6.

Kittitas Chute - Observations on Kittitas chute were not taken by Hall, but he used Kittitas chute data also in his analysis. Tests were actually conducted by C. L. Thomas of U.S.P.R. This chute is a wasteway from Kittitas main canal located on Yakima project and is 397 m long with a vertical drop of 104 m. Its width in most of the reach is 2.44 m. It has only a few vertical and horizontal curves. Velocity observations at Kittitas chute were taken electrically using salt as a conductor.

### Theoretical Considerations

Hall has made following assumptions in developing theory of flow in chutes,

1. The value of Manning's roughness coefficient 'n' is constant for the particular type of the material of which the chute is constructed.
2. The air in and above the water causes no additional loss in energy, the reduction of specific gravity compensating for the added area.
3. For computations, a computed hydraulic radius can be used,

$$R_c = \frac{Q}{V P_c} \quad \dots \quad (4)$$

with a smaller value of n than the usual.

Here Q = discharge

V = observed velocity

$P_c$  = computed wetted perimeter of the section of water only  
 $A_c = Q/V$

4. The velocity head ( $h_v$ ) computed from the mean velocity can be used without substantial error.

The value of roughness coefficient n can be computed

from the energy gradient  $S$  using the Manning's formula,

$$S = \frac{n^2 V_0^2}{(R_0)^{4/3}} \quad \dots \quad (5)$$

$R_0$  being the observed hydraulic radius and  $V_0$  the observed velocity.

If  $R_c$  is used instead of  $R_0$ , a different value of  $n$ ,  $n_c$ , must be used given by,

$$n_c = n \left( \frac{R_c}{R_0} \right)^{2/3} \quad \dots \quad (6)$$

Since  $R_c$  is always less than  $R_0$ ,  $n_c$  obviously will be less than  $n$ .

Now applying Bernoulli's theorem with reference to Fig.2.

$$h_E = h_Z - L \sin \theta + Y \cos \theta + \frac{\alpha_a V^2}{2g} \quad \dots \quad (7)$$

$\alpha_a$  being velocity head coefficient given by

$$\alpha_a = \frac{\int v^3 dA}{V^3 A} \quad \text{and} \quad h_v = \frac{\alpha_a V^2}{2g} \quad \dots \quad (8)$$

in which  $v$  = velocity through an elemental area  $dA$  and  $V$  is the average observed velocity. Now differentiating w.r.t. 'L',

$$\frac{dh_E}{dL} = - \sin \theta + \cos \theta \frac{dY}{dL} + \frac{\alpha_a V}{g} \frac{dV}{dL}$$

In a rectangular channel we can substitute the computed depth

$Y_c = p_w Y$  for the value of  $Y$ ,  $p_w$  being the ratio of water in a mixture of air and water. The discharge per unit width  $q = VY_c$ .

Now since  $q$  remains constant from section to section,

$$Y_c dV + V dY_c = 0, \quad \therefore dY_c = - Y_c \frac{dV}{V} = - q \frac{dV}{V^2}$$

and hence we obtain,

$$-S = \frac{dh_E}{dL} = -\sin \theta - \frac{\cos \theta}{V^3} \alpha \cdot \frac{dV}{dL} + \frac{\alpha a V}{g} \frac{dV}{dL}$$

Solving for  $\frac{dL}{dV}$  we obtain,

$$\frac{dL}{dV} = \frac{\frac{\alpha a V}{g} - \frac{q}{V^3} \cos \theta}{\sin \theta - S}$$

or 
$$\frac{dL}{dV} = \frac{\frac{\alpha a V}{g} - \frac{q}{V^3} \cos \theta}{\sin \theta - \frac{n_c^3 V^2}{R_c^{4/3}}} \dots (9)$$

This is the basic equation for flow in steep rectangular chutes. In this equation however the value of  $n_c$  is dependent on  $p_w$ , the ratio of water in an air water mixture because  $n_c = n \left( \frac{R_c}{R_o} \right)^{2/3}$ .

By plotting experimental data Hall innovated a linear relationship between kinetic flow factor  $\frac{V^2}{gR_c}$  and air to water ratio  $\frac{1-p_w}{p_w}$  as below,

$$\frac{1-p_w}{p_w} = K \frac{V^2}{gR_c} - K_1 \dots (10)$$

assuming  $K_1 = 0$

$$p_w = \frac{1}{1 + \frac{KV^2}{gR_c}} \dots (11)$$

again if  $b_f$  = width of channel then,

$$R_c = \frac{b_f \frac{q}{V}}{b_f + \frac{2q}{V}} = \frac{q}{V + \frac{2q}{b_f}}, \text{ and putting } B = \frac{2q}{b_f} \text{ for}$$

simplicity of expression

$$R_c = \frac{q}{V + B}$$

Similarly we may obtain  $R_0 = \frac{q}{p_w V + P}$ , hence,

$$\frac{R_c}{R_0} = \frac{p_w V + P}{V + P} \quad \dots \quad (12)$$

Substituting (11) and (12) in eqn. (6),

$$n_c = \eta \left[ \frac{1 + \frac{B}{q} \cdot \frac{KV^2}{g}}{1 + \frac{KV^2}{g} \left( \frac{V+B}{q} \right)} \right]^{2/3} \quad \dots \quad (13)$$

Equations (11) and (13) constitute basic formulae for the solution of problems of air entrainment in spillway chutes. The use of value of  $n_c$  from eqn. (13) in eqn. (9) affords a rational theoretical solution for flow in rectangular chutes.

The ratio  $\frac{1 - p_w}{p_w}$  has been plotted against  $\frac{V^2}{9R_c}$  in fig.7. Straight line fit has been obtained in all cases but there is a considerable scatter of experimental data.

According to Warren DeLapp<sup>10</sup> the scatter in fig.7 is due to the fact that Hall tried to find a general solution for a wide variety of cases. An examination of data shows that the percentage of air is greater for retarded than for accelerated flow for a given  $\frac{V^2}{9R_c}$ . Also flow at variation in horizontal and vertical curves introduces new variables. So best thing would be to take the data corresponding to points where the flow is in equilibrium. Apart from the Froude number the air entrained should also depend on the channel roughness which would affect the agitation of flow. The form of function suggested by Lapp is,

$$\frac{Q_{aw}}{Q_w} = K_L F \quad \dots \quad (14)$$

in which  $Q_{aw}$  is the quantity of air and water,  $Q_w$  of water alone, and  $F$  is the Froude number  $\frac{V}{\sqrt{gY_u}}$  and  $K_L$  the coefficient whose

value depends on the roughness of the slope (experimentally determined equal to 0.178 for Rapid flume and 0.227 for Kittitas chute).

$$\text{Put } \frac{Q_{aw}}{Q_w} = \frac{b_f Y_u V}{b_f q_w}$$

Where  $Y_u$  = depth of air water flow and  
 $q_w$  = water flow per unit width

$$\text{Therefore, } \frac{Y_u V}{q_w} = K_L \frac{V}{\sqrt{g} Y_u}$$

$$\text{so that } Y_u = K_L^{2/3} \left( \frac{q_w^2}{g} \right)^{1/3} \quad \dots \quad (15)$$

Douma<sup>11</sup> suggested the use of

$$V = \frac{N}{n} R^{2/3} S^{1/2} \quad \dots \quad (16)$$

instead of using  $V = \frac{1}{n} R^{2/3} S^{1/2}$  as done by Hall.  $N$  will vary and will be 1 for non-aerated flow. With this eqn. (9) becomes,

$$\frac{dL}{dV} = \frac{\frac{\alpha V}{g} - \frac{q \cos \theta}{V^2}}{\sin \theta - \frac{n^2 V^3}{N^2 R_o^{4/3}}} \quad \dots \quad (17)$$

In this  $R_o$  and  $N$  are functions of velocity and air content. The equation can be solved by determining expressions for  $R_o$  and  $N$  in terms of  $V$  and known quantities. Douma plotted percentage of air  $C$  against  $\frac{V^3}{gR_o}$ . The average of all points is approximated by  $C^2 = 0.002 \frac{V^3}{gR_o} - 0.01$  ..... (18)

This gives  $C = 0$  at  $V = \sqrt{5gR_o}$ . Next the data for Hat creek and Kittitas chutes were used to evaluate  $N$ . This showed that  $n$  increases with  $C$  giving

$$n = \frac{0.006}{0.6 - C^2} \quad \dots \quad (19)$$

This equation roughly gives  $n = 0.010$  for smooth concrete chutes for non-aerated flow. Taking this value of 'n' the relationship appears to be

$$N = 1 - 1.67 C^2 \quad \dots \quad (20)$$

Thus the maximum value of  $N$  is 1 for no air entrainment and decreases as air proportion increases.

Hall also observed that the initial entrainment of air depends to a great extent on entrance conditions. With a well designed entrance the water accelerates uniformly, gradually drawing air into the water prism. This insufflation first begins on the side walls and then spreads gradually into the section.

### 2.3 STUDIES ON NATURAL CHUTES IN YUGOSLAVIA<sup>18</sup>

V.Jevdjevich and L.Levin have reported field studies on Mostarsko Blato and Imotska Polje flumes in Yugoslavia. Air water mixture velocity distribution and the distribution of velocity of the air above it at Mostarsko Blato are shown in fig. 8 for a discharge of 24.4 cumec. It can be seen that while the mean velocity of air water mixture is 29.5 m/sec, bulk of air movement is at a speed of 3 to 5 m per sec and the gradient of velocity at the interface is very high.

#### Effect of Aeration on Manning's Coefficient

Manning's coefficient is generally computed from the formula,  $n = \frac{1}{\sqrt{V}} R^{2/3} S^{1/2}$ . If  $n$  is the resistance coefficient corresponding to aerated flow and  $n_0$  corresponding to non-aerated flow, it is observed that  $n < n_0$ . In fact if density of air water mixture or water factor is denoted by  $p_w$  then 'n' decreases with decrease of water factor at boundary  $p_{wb}$ . This is apparent from fig.11 which gives variation of 'n' with ' $p_{wb}$ ' for chutes at Mostarsko Blato

and Gizeldon.

A plaster print was taken of the bottom of Mostarsko Blato made of stone lining. Its profile indicated a coefficient of roughness for non-aerated flow  $n_0 = 0.019 \approx 0.020$ . However on the basis of measurements at the 3 m wide Mostarsko Blato for discharges ranging from 3.9 to 18.3 cumec, it was obtained that  $n = 0.0135 \rightarrow 0.0145$  i.e. it was decreased by about 30% which is attributed to aeration.

#### Froude Number and Manning's Coefficient

Jevdjevich and Levin have quoted that for small discharges and low Froude numbers the effect of super-rapid flow on friction is to increase the value of  $n$ . Friction losses increase suddenly at Froude number  $F_r \approx 2$  and  $n > n_0$ . However when aeration starts, which as already mentioned, acts, so as to make  $n < n_0$ , the two influences partly compensate each other. At low  $F_r$ , the first influence predominates and  $n$  increases; at high values of  $F_r$ , the effect of aeration predominates and the value of  $n$  goes below  $n_0$  (Fig. 9).

At the rapid flume of Imotsko Polje measurements were taken for super rapid flow. The chute is made of smooth concrete, with a bottom slope  $S = 0.555$  and consists of three parallel straight lined channels each 2.34 m wide. For a discharge of 1.15 cumec, the mean velocity measured by colorimetric method amounted to 8.0 m/sec and the regime was super-rapid and very aerated. Under these conditions the roughness coefficient ' $n$ ' was computed to be 0.0142 which is a normal value for non-aerated smooth concrete surface. It is inferred that this point is to be found at the Froude number for which the two opposite influences compensate each other. At Imotsko Polje, Froude number  $F_r = \frac{V}{\sqrt{gR}}$  at this point was computed

to be 10.6.

Relationship Between Mean Water Factor and Flow Parameters

Jevdjevich and Levin argue that the water factor depends on the degree of agitation of flow or in other words on the mean velocity  $V$  and the hydraulic radius  $R$ . These can be combined into a dimensionless number

$$F_r = \frac{V}{\sqrt{gR}} \quad \dots \quad (21)$$

The water factor should also depend on roughness of the channel which is defined by the coefficient 'n'. Since this is not dimensionless, a function is defined as

$$\psi = \frac{n_0}{R^{1/6}} \sqrt{g} \quad \dots \quad (22)$$

Also velocity distribution and water factor distribution along the depth must also influence the mean water factor of the mixture. Forming a dimensionless number of the form of Coriolis coefficient for aerated flows, we get ;

$$\alpha_a = \frac{\int_0^Y p_w v^3 dy}{p_{wm} V_m^3 Y} \quad \dots \quad (23)$$

Where suffix 'm' stands for mean values.

Figure 10 shows the distribution of velocity and water factor at Mostarsko Blato for discharges of 3.9 and 10.4 cumec.  $V$ ,  $R$ , and  $p_w$  were determined experimentally and  $F_r$  and  $\psi$ , determined on the basis of these.

Jevdjevich and Levin have proposed the following relationship embodying various dimensionless parameters developed in equations (21), (22) and (23),



$$\frac{1 - p_w}{p_w} = A F_r^3 \psi \alpha_a \quad \dots \quad (24)$$

The proportionality constant A is shown in fig.16. It is seen that it is relatively a constant having a value of 0.175 with a deviation of 10 percent.

## CHAPTER - 3

### REVIEW OF LABORATORY STUDIES

#### 3.0 INTRODUCTION

Many a times the observations in the field present problems, which, if not properly taken care of, can vitiate the results. All the more, to decipher the effect of various parameters on the air entrainment phenomenon, it is necessary to conduct laboratory studies. These researches also help to build up the back-ground theory for proper understanding of the phenomenon. In the past few decades studies on specially constructed laboratory flumes have been conducted in various research laboratories throughout the world. These include the work done in the Neyrpic Laboratory in France, the Naples University in Italy, the St. Anthony Falls Laboratory in U.S.A. and in India at the Central Water and Power Research Station at Poona and also in the Hydraulics Laboratory of Indian Institute of Science at Bangalore. These studies are described in this chapter.

#### 3.1 STUDIES IN THE NEYRPIC LABORATORY, FRANCE<sup>14</sup>

G. Halbronn, R. Durand and G. Cohen De Lara have reported the work done in connection with air entrainment at Neyrpic Laboratory, France. The flume of width 0.5 m was placed on an adjustable slope platform. The discharge entering the flume was measured by a venturimeter installed in the supply pipe and arrangements were made to regulate the gate opening at the inlet end of flume such that the flow attains, from the outset, an average velocity which is in the vicinity of the mean uniform regime velocity.

##### Measurements of Air Concentration

A gage consisting of two 0.15 mm enamelled constantan wires

wound in a double helix around a third rectilinear supporting wire is used. The outside of the coils of the two wires is kept bare over a length of 5 mm. If there is a difference of potential between these wires, the circuit is completed through the electrolyte. The air concentration  $C$  is linearly related to  $R_0/R$  where  $R_0$  is the resistance in clear water and  $R$  in the air water mixture.

### Measurements of Velocities

Velocities were measured by employing a dynamic pressure tapping connected to a water manometer. Arrangements were made to prevent entry of air into the connecting pipes. To correct for influence of tapping on flow a coefficient  $t_p$  is used which is the ratio of the air concentration at the tapping intake to the concentration when the obstacle is removed ( $0 \leq t_p \leq 1$ ). The overpressure  $h$  in terms of head of water is related to the velocity  $v$  of the water at the tapping by

$$h = (1 - t_p \cdot C) \frac{v^2}{2g} \quad \dots \quad (25)$$

Also it has been seen that  $t_p$  is nearly unity when the ratio of the bubble diameter to the measuring tube diameter is small.

### Determination of Uniform Regime

By uniform regime is meant that condition of air water mixture flow for which the curves of velocity distribution and air-concentration distribution are the same at any two sections of the flume. This was tested by comparing the air concentration and velocity distributions in the median vertical plane at two sections 2.1 m apart with a discharge of 100 litres per second.

### Qualitative Observations

Stroboscopic flow observations show that generally the bubbles are spherical, their diameter is about 1.5 mm except near the bottom where the extremely minute particles are present. The air concentration appears to be higher near the walls than in the central region. Moreover the bubbles are larger in the central region. Their diameter<sup>s</sup> range from 4 mm to 5 mm.

### Discussion of Results

Figures 12 and 13 show typical distribution of air concentration and velocities respectively for a cross/section of a flume for a discharge of 100 litres/sec. Figures 14 and 15 show the curves of air concentration and velocity distribution in the vertical median plane for six discharges ranging from 60 lit/sec to 182 lit/sec investigated on a flume slope of  $14^{\circ}$ . Due to a slight distortion of canal the zone of the maximum velocities is a bit deviated towards the right hand wall depending on the discharge. This is perhaps responsible for a lack of continuity in the air concentration profile.

All the air concentration curves show a break for concentrations of about 60%. It may be at the transition from the emulsion zone (air bubbles in water) to ejection zone (drops of water in air). In fact the air bubbles carried up into the upper part of emulsion zone are spherical with practically the same diameter and the maximum degree of compactness of such a sphere system is also about 60%. If the air concentration tends to rise above 60% the bubbles which are squashed up against each other, unite and the water which surrounds them changes into drops. This is the transition from the emulsion to the ejection stage.

The depths corresponding to these zones were also obtained directly. The data given by a static pressure tapping placed in the flow were measured by a micromanometer, and in the droplet zone only the atmospheric pressure was measured. The curve obtained by investigations along a vertical line also presents a break at the passage from one zone to another. It is therefore confirmed that for a  $14^\circ$  slope the transition from emulsion to droplet zone corresponds to an air concentration of 60% irrespective of the discharge.

### 3.2 STUDIES IN THE LABORATORY OF UNIVERSITY OF NAPLES, ITALY<sup>33,34</sup>

M. Viparelli has reported the work done at Naples. Initial experiments were done on a flume of 1:1 slope which was later on given two other slopes of  $23^\circ 30'$  and  $11^\circ 20'$ . The flume was rectangular in section, 0.2 m wide and having very smooth concrete walls. The length of flume was sufficient to reach at its lower end conditions of uniform flow in all cases.

#### Experiments at 1:1 Slope<sup>33</sup>

The following quantities were considered in the analysis,

- 1) The velocity ' $v$ ' at a point
- 2) The percentage ' $p_w$ ' of water present in a unit volume
- 3) The discharge ' $u_q$ ' through the unit area of cross-section
- 4) The ratio  $p'_w$  of the water discharge rate  $u'_q$  to the rate of mixture  $u'_q$  through a unit area.

The following measurements were taken,

- 1) Head ' $h$ ' on the tip of Pitot tube connected to a manometer.
- 2) Water discharge  $q_s(\gamma)$ , flowing through a unit width of section and above a height  $\gamma$  from the bed of flume. This was measured by using an open sampler as shown in fig. 17. From this  $u_q$  is computed as

$$u_q = \frac{q_s(\gamma) - q_s(\gamma + \Delta\gamma)}{\Delta\gamma} \dots (26)$$

3) Ratio  $\beta$  between air and water discharge rates syphoned by the current in a closed vessel in which a depression  $\Delta$  was maintained (Fig. 20).  $p'_w$  was then obtained by the formula,

$$p'_w = \frac{1}{1 + \beta} \dots (27)$$

4) The percentage  $p_w$  of water present in a unit volume of mixture by using an electric sampler with small plates and on the basis of the principle of change in resistivity of mixture as compared to that of clean water.

Curves of the percentage  $p_w$  of water present in a unit volume were plotted as in fig. 19. These curves alongwith the visual observations of flow subscribe to the division of flow into three layers viz.,

- (1) Bottom layers of predominantly water flow with little quantities of air bubbles.
- (2) Intermediate layers of air and water flow.
- (3) Upper layers of air with water drops in movement.

Considering the bottom layers of flow,

$$u_q = p'_w v \dots (28)$$

also  $p_w \cdot \gamma_w \cdot \frac{v^2}{2g} = \gamma_w h,$

which gives,  $v = \frac{1}{\sqrt{p_w}} \cdot \sqrt{2gh} \dots (29)$

Combining equations (28) and (29) we get

$$u_q = \frac{p'_w}{\sqrt{p_w}} \cdot \sqrt{2gh} \dots (30)$$

Near bottom  $p'_w$  and  $p_w$  are little different from unity, hence we may write

$$u_q = \sqrt{2gh} \quad \dots \quad (31)$$

This was confirmed by experimental values also, as in fig. 18 wherefrom it is seen that in the bottom layers the curves of  $u_q$  and  $\sqrt{2gh}$  v.s.  $\log y$  are more or less coincident. Again as far as  $p'_w$  differs little from unity

$$v = u_q = \sqrt{2gh} \quad \dots \quad (32)$$

From fig. 18 it is also seen that the plot of  $\sqrt{2gh}$  and  $\log y$  is disposed along a straight line upto a certain height 'y' above bottom which increases with water discharge. From this it can be concluded that in the bottom layers the distribution follows the logarithmic law of turbulence theory.

In the upper layers of flow the experimental points place themselves according to two straight lines almost parallel to each other (Fig. 18), one for  $(u_q, \log y)$  and the other for  $(\sqrt{2gh}, \log y)$ . Dynamic pressure due to air velocity being negligible, head  $h$  may be considered to be due to the impingement of water drops on the Pilot tube. As the number and average values of such impulses (mass x velocity of impinging drops) are proportional to the water mass that cross unit area, that is  $u_q$ , the direction almost parallel of the two curves in the upper layers indicate that the average velocity of water drops is almost constant.

Further when in upper layers of flow values of  $\log u_q$  were plotted against  $y$ , the points disposed on parabolas with  $u_q$  decreasing as  $y$  increased. This indicates that in upper layers the number of drops decrease according to the law of normal probability. This may be expected as the drops are thrown about because of the random turbulent fluctuations.

From the shape of the curves it was also seen that the greatest velocity in the current is attained in the layers where

air and water are in almost equal quantities.

Near the bottom it was also seen that  $p'_w > p_w$  which indicates that water is moving faster than air. This has been interpreted by Viparelli to mean that air moves remarkably at random following the fluctuations of the turbulence, instead of having an actual slip with respect to the surrounding water particles. However in most of the studies and in design procedure the water and air are taken to move together at the same velocity.

### Further Experiments on Flatter Slopes<sup>34</sup>

Further experiments were conducted by giving the flume flatter slopes of  $23^{\circ}30'$  and  $11^{\circ}20'$  successively. Values of  $h$ ,  $q_s(y)$ , and  $\beta$  as already defined were measured for each slope for discharges of 10, 20, 30, and 40 litres/sec. Complete series of observations were taken along a normal to the bottom on the axis of the channel near lower end.

When values of  $h$  were plotted against corresponding values of  $y$  for any particular slope and discharge, a curve exhibiting a maxima  $h_{max}$  resulted (Fig. 23). Corresponding value of  $y$  is designated as  $d_m$ .

Values of  $q'_s(y) = q_s(0) - \int_0^y \sqrt{2gh} \, dy$  were computed and compared with values of  $q_s(y)$  obtained by direct measurements. It was found that  $q'_s(y)$  and  $q_s(y)$  agree very closely for  $y < d_m$  and further in this range  $\beta$  is very small, being one to two percent. Thus for  $y < d_m$  air contents are small and  $\sqrt{2gh}$  can be taken as the velocity of the current.

In the upper layers Viparelli assumed the velocity of water drops  $v = \sqrt{2gh}_{max}$ . The impulses on Pitot tube in a unit time are  $\frac{\gamma_w}{g} u_q \cdot v$ . The simplest relation that may be expected



between dynamic pressure  $\gamma_w h$  and impulses on Pitot tube per unit time  $\frac{\gamma_w}{g} u_q \cdot v$  may be taken as one of direct proportionality

$$\gamma_w h \propto \frac{\gamma_w}{g} u_q \cdot v$$

or  $gh \propto u_q \cdot v$

This proportionality may also be written in the form

$$\frac{\sqrt{2gh}}{u_q} \propto \sqrt{\frac{v}{u_q}} \quad \dots \quad (33)$$

Values of  $\frac{\sqrt{2gh}}{u_q}$  and  $\sqrt{\frac{v}{u_q}}$  calculated from experimental data for different slopes and discharges were plotted and found to exhibit a linear relationship

$$\frac{\sqrt{2gh}}{u_q} = A + B \sqrt{\left(\frac{v}{u_q}\right)} \quad \dots \quad (34)$$

Where A and B are constants varying with experiments. One such plot has been shown for a discharge of 40 litres/sec for all the three slopes investigated in fig.21(a).

### Discussion of Results

As already indicated the flow is to be treated separately for layers near the bottom and upper layers.

#### Layers Near the Bottom

It has already been indicated that in bottom layers velocity distribution follows logarithmic law. Logarithmic distribution for smooth boundaries as at Naples is given by

$$\frac{v}{\sqrt{J_0/f}} = a + \frac{2.3}{K} \log_{10} \frac{\sqrt{J_0/\rho}}{U} \quad \dots \quad (35)$$

where  $J_0$  is wall shear and  $\rho$  is mass density of fluid.  $U$  is kinematic viscosity. Average value of constant  $a = 5.5$  and that of Von Karman's universal constant  $K = 0.40$  in case of non-aerated

flows. For  $y < d_m$  experimental values  $\sqrt{2gh}$  plotted against  $y$  in a semilogarithmic diagram show a linear tendency; but it is difficult to determine numerical coefficients of eqn. 35 in aerated flows because  $\sqrt{\mathcal{T}_0/\rho}$  is uncertain. The value of wall shear  $\mathcal{T}_0$  is deduced by using the component of the weight of unit length of current along axis of channel. Here the weight that may be taken can be (1) that of current of height  $d_m$  or (2) to this can be added partly or wholly that of water drops in upper layers. For each discharge and slope coefficient 'a' and Von Karman's constant  $K$  were computed giving  $\mathcal{T}_0$  the two values obtained assuming respectively only the weight of current of height  $d_m$  (hypothesis-1) or including also the gravity of all water drops (hypothesis-2). It was seen particularly with hypothesis-1 that average value of  $K$  is less than 0.40. Similar results were obtained by some investigators in case of currents of sediment laden water. It was hypothesized that  $K < 0.40$  because sediment suspended in water damps out turbulence. The effect of suspended air bubbles thus, is also seen to be similar.

Further Manning's coefficient was computed using for velocity the value equal to the discharge passing below the height  $d_m$  divided by the area of channel below height  $d_m$ . The Manning's coefficient is found to oscillate between 0.0062 and 0.0072 which agree well with the nature of boundary. Viparelli therefore concludes that water flow in layers near bottom follows the normal laws of current.

#### Flow in Upper Layers

Water drops jump in air due to the action of random fluctuations of turbulence and are distributed in the air according to the normal law of probability. The drops conserve the velocity

$v = \sqrt{2gh_{\max}}$  of layers from which they depart. Hence not only the number of drops but also water discharge per unit area for the upper layers ( $y > d_m$ ) is distributed according to the law of normal probability. This is evident by the plots of the ratios  $P = \frac{100 q_s(y)}{2 q_s(d_m)}$  against corresponding  $\frac{y-d_m}{h_{\max}}$  on a probability paper. The points were found to dispose more or less along straight lines. One such plot has been shown for a discharge of 40 litres/sec for all the three slopes investigated in fig. 21(b).

Viparelli has also given an expression for the discharge per unit area in upper layers as

$$u_q = v e^{-\frac{1}{2} \left( \frac{y-d_m}{\sigma h_{\max}} \right)^2} \dots (36)$$

Where  $\sigma$ , the standard deviation varies between 0.0018 to 0.0025 according to experimental results at Naples for the smooth concrete flume.

#### Gizeldon Chute Experiments

Viparelli also analysed the results of experiments done on the spillway of Gizeldon Plant in U.S.S.R. and reported by Nitchiporovich. The chute is a rectangular wooden channel 6 m wide and 23.7 m long with an inclination of  $32^{\circ}20'$  with horizontal. The experiments were conducted with discharges of 2.58, 4.48, 5.23 and 7.62 cumec. The walls of this chute are not smooth and so the normal distribution of velocity was assumed to follow the relationship for rough boundaries,

$$\frac{v}{\sqrt{\mathcal{T}_0/\rho}} = b + \frac{2.3}{K} \log_{10} \frac{y}{\epsilon} \dots (37)$$

where average values of  $b$  and  $K$  are 8.48 and 0.40 respectively and  $\epsilon$  is a measure of roughness of walls. If values of  $\mathcal{T}_0$  are calculated according to weight of current of height  $d_m$  then

from the slope of straight lines on which the point  $(\sqrt{2gh}, y)$  dispose on semilogarithmic diagrams, values of  $K$  less than 0.40 ( a good average  $K = 0.35$ ) are obtained like those found for smooth walls at Naples.

Manning's coefficient was also determined considering the flow in layers below height  $d_m$  and discharge  $q = \int_0^{d_m} \sqrt{2gh} \cdot dy$ . They oscillate between 0.009 and 0.010 in good agreement with nature of wall surface.

When upper layers are considered, relations of the type

$$\frac{\sqrt{2gh}}{u_q} = A + B \sqrt{\left(\frac{v}{u_q}\right)}$$

should be expected. However since Nitchiporovich did not measure  $u_q$  Veparelli computed  $u_q$  employing eqn. (36), using trial values of  $\sigma$  until corresponding values of  $\left(\frac{\sqrt{2gh}}{u_q}, \sqrt{\left(\frac{v}{u_q}\right)}\right)$  plotted along straight lines. Figure 22 shows one such plot. The  $\sigma$  values were found to oscillate between 0.0020 to 0.0040. They are a little higher than those for laboratory flume with smooth walls. At Naples also when experiments were conducted with artificially roughened bottom floor  $\sigma$  was found to have a value equal to 0.004 approximately. Hence Veparelli recommends to compute  $u_q$  in upper layers with the help of equation (36) using  $\sigma = 0.0025$  for smooth and  $\sigma = 0.004$  for rough walls.

### 3.3 STUDIES AT THE ST. ANTHONY FALLS LABORATORY, U.S.A. <sup>31,30,1</sup>

The experiments were conducted in a special laboratory channel 15 m long and 0.45 m wide. This width was seen to be enough for the flow depths used in the sense that the character of the flow was two dimensional for a few centimeters near the centre of the flume. The inlet velocity was adjusted to be approximately the terminal velocity for the given slope and

discharge so that the flow could be studied independently of large accelerative or decelerative effects.

### Velocity Observations

Velocity observations were taken by employing an electro-chemical device which timed the travel of minute salt water cloudlets injected into the air water mixture. The passage of ionized cloudlet is detected by electrodes fixed 75 mm apart in the flow path. Traverses were first obtained for non-aerated flows to obtain Manning's 'n' values for the flume surface which was of painted steel. Manning's equation for a unit breadth of channel may be written down as

$$V_n = \frac{1}{n} d_n^{2/3} S^{1/2}$$

This when combined with equation of continuity,

$$q = V_n \cdot d_n \quad \text{yields,}$$

$$V_n = \left( \frac{1}{n} \right)^{0.6} q^{0.4} S^{0.3} \quad \dots \quad (38)$$

Where  $V_n$  = mean velocity in non-aerated flow (m/sec)

$d_n$  = mean depth in non-aerated flow (m)

$q$  = water discharge rate (cumec )

$S$  = slope of channel i.e.  $\sin \alpha$

Having obtained value of  $n$  from non-aerated flow data  $V_n$  was computed for  $q = 0.18$  cumec for different slopes and the values were compared with mean velocities in aerated flows obtained by averaging the observed velocity distributions along the centre line vertical (Fig. 27). It was found that the predicted mean velocities of non-aerated flow were too low as compared to the measured mean velocities for aerated flow.

### Air Concentration Observations

Air concentration 'C' at any point of flow was measured by electrical air concentration meter which basically measures the difference between the conductivity of a mixture of air and water and the conductivity of water alone. Concentration contours for a section 13.5 m from inlet are shown in fig. 25. These contours are seen to be considerably higher near the side walls than in the central region. This side wall effect is especially noticeable before aeration begins in the central region; aeration at the sides is initiated by the turbulence from the side wall boundary at the water surface which thus appears as white water sooner. The flat contours in the central region are indicative of the two dimensional character of flow there.

The concentration curves along centre line vertical for various flume angles at 13.5 m from inlet at constant discharge are shown in fig. 26. The mean air concentrations when computed from these curves were found to increase with increasing flume angles.

### Artificially Roughened Channels<sup>30</sup>

Further and more detailed studies were conducted after artificially roughening the channel bed by laying a commercial non-slip fabric coated with granular particles of mean size 0.7 mm at a mean spacing of 1 mm. The bed was thus considerably rougher than the painted steel side walls of the channel.

Experiments were made for slopes from  $7.5^\circ$  to  $75^\circ$  at  $7.5^\circ$  intervals and discharge varied from 0.062 to 0.272 cumec and in some cases upto 0.425 cumec. Measurements of air concentration were made at 13.5 m from inlet along a centre line normal at 3 mm interval starting from a point at 6 mm from bed and upto a

point which was completely out of flow i.e. where meter registered zero air concentration.

### Definitions of Depth and Concentration Parameters

For further discussions and analysis of data it is essential to define certain depth and air concentration parameters as given below,

$c$  = air concentration i.e. volume of air per unit volume of air water mixture

$y$  = distance from and normal to the channel bed

$\bar{d}$  = mean depth of flow that would exist if all of the entrained air was removed up to the highest point where water is found, thus,

$$\bar{d} = \int_0^{\infty} (1 - c) dy$$

In other words this is the depth of a non-aerated flow of a given discharge with a velocity equal to that of air entrained flow

$d_u$  = value of  $y$  where  $c$  has some preassigned value say 0.99. This depth encompasses about 98 to 99% of all the water and consequently may be taken to represent an upper limit for water

$d_T$  = value of  $y$  where the transition occurs from lower region of flow in which air bubbles are suspended in water to upper region of flow in which water droplets move in air

$\bar{c}$  = mean air concentration in the vertical in the entire flow (based on  $d_u$ )

$$= \frac{1}{d_u} \int_0^{d_u} c dy$$

$\bar{c}_T$  = mean air concentration in the vertical in the lower region (based on  $d_T$ )

$$= \frac{1}{d_T} \int_0^{d_T} c dy$$

Other terms will be defined as and when they occur.

### Distribution of Air Concentration

Observations by means of instruments indicate that two

regions develop in self-aerated flow;

(1) an upper region of heterogeneous clumps, globules and droplets of water ejected from the flowing stream at more or less arbitrary velocities and

(2) a lower region consisting of air bubbles distributed through the flow by turbulent transfer.

Between the two regions is a transition zone defined by a transition depth that is a fluctuating surface <sup>n</sup>necessarily at a statistical mean elevation above the channel bottom. The two regions are treated separately.

#### Distribution of Air in Upper Region

Assuming turbulent velocity fluctuations in a direction normal to bed to have a random distribution, the frequency  $f(y')$  of particles projected upwards to the distance  $y'$  above the transition may be taken as half the Gaussian,

$$f(y') = \frac{2}{\sigma\sqrt{2\pi}} e^{-\frac{1}{2} \left( \frac{y'}{\sigma} \right)^2} \dots \quad (39)$$

where  $\sigma$  is the standard deviation of the Gaussian distribution.

The factor 2 is used to indicate that only particles being projected in the outward direction are being considered so that  $\int_0^{\infty} f(y') dy' = 1$ . Thus proportion of all particles leaving a unit area of the transitional surface and reaching or passing through a corresponding area at  $y'$  is

$$P(y') = \frac{2}{\sigma\sqrt{2\pi}} \int_{y'}^{\infty} e^{-\frac{1}{2} (y'/\sigma)^2} dy' \dots \quad (40)$$

This may be taken proportional to the water concentration  $(1-c)$ .

Thus the air concentration 'c' at  $y'$  is given in terms of concentration  $c_T$  as



into (44),

$$Cv_b = \beta K \sqrt{\left(\frac{T_0}{\rho}\right)} \left(\frac{d_T - y}{d_T}\right) \cdot y \frac{dC}{dy} ,$$

which on integration yields,

$$C = C_{\Phi} \left(\frac{y}{d_T - y}\right)^z \dots (46)$$

in which,

$$z = \frac{V_b}{\beta K \sqrt{T_0/\rho}} = \frac{V_b}{\beta K V_*} \dots (47)$$

and  $C_{\Phi}$  is a constant whose value is the concentration at  $y = \frac{d_T}{2}$ .

### Application to Experimental Data

Equations (41) and (46) describe the air concentration distribution in an open channel. The constants involved can be determined empirically for a given channel, from the observed curves for air concentration.

Firstly the transition depth  $d_T$  and the air concentration  $C_T$  at that depth were determined for a particular discharge and slope from a plot of  $C$  in terms of  $y$ . The point where  $\frac{dC}{dy}$  is maximum is graphically located as in fig. 28(a). The corresponding value of  $d_T$  and  $C_T$  are noted. Using this value of  $C_T$ , the ratio  $\frac{1 - C}{2(1 - C_T)}$  was plotted as a function of  $y$  on probability paper on which a cumulative Gaussian distribution plots as a straight line. Figure 28(b) shows one such plot in the upper region of flow. It is apparent from this that the concentrations possess a cumulative Gaussian distribution.

In the region of flow below  $d_T$  equation (46) indicated that  $C$  is a function of  $\frac{y}{d_T - y}$  and should on a logarithmic plot result in a straight line where slope is equal to the exponent  $z$  and  $C_{\Phi}$  is the value of  $C$  at  $\frac{y}{d_T - y} = 1$ . The logarithmic plot of experimental data as in fig 28(c) shows excellent agreement

$$\frac{1 - c}{1 - c_T} = \frac{2}{\sigma\sqrt{2\pi}} \int_0^{\infty} \frac{1}{e^{\frac{1}{2}(y'/\sigma)^2}} dy' \quad \dots \quad (41)$$

and the gradient of concentration is given by

$$\frac{dc}{dy} = \frac{2(1 - c_T)}{\sigma\sqrt{2\pi}} \frac{-1}{e^{\frac{1}{2}(y'/\sigma)^2}} \quad \dots \quad (42)$$

From which we observe that air concentration gradient  $\frac{dc}{dy}$  is maximum when  $y' = 0$  and the value  $\left(\frac{dc}{dy}\right)_{\max} = \frac{2(1 - c_T)}{\sigma\sqrt{2\pi}}$  (43)

and this occurs where  $c = c_T$  and  $y = d_T$  /

### Distribution of Air in Lower Region

The air entrained in the lower region below the transition depth, is in a state of statistical equilibrium between the force of buoyancy of air bubbles and the mixing effect due to turbulence. Such an equilibrium is described by the equation,

$$- CV_b + \epsilon_b \frac{dC}{dy} = 0 \quad \dots \quad (44)$$

where  $V_b$  = rising velocity of air bubbles and is being considered negative

$\epsilon_b$  = mixing coefficient for air bubble transfer. This may be assumed proportional to momentum mixing coefficient (as is done in sedimentation theory). Thus  $\epsilon_b = \beta \epsilon_m$ .

And assuming a Karman type logarithmic velocity profile with shear linearly distributed along the vertical, Straub and Anderson have arrived at

$$\epsilon_b = \beta K \sqrt{\tau_0/\rho} \left(\frac{d_T - y}{d_T}\right) y \quad \dots \quad (45)$$

where  $K$  = Karman's universal constant

$\tau_0$  = boundary shear at bed

$\rho$  = mass density of fluid.

$\sqrt{\tau_0/\rho}$  which has dimensions of velocity is generally expressed as shear velocity  $V_*$ . Substituting the value of  $\epsilon_b$  from (45)

into (44),

$$CV_b = \beta K \sqrt{\left(\frac{\tau_0}{\rho}\right)} \left(\frac{d_T - y}{d_T}\right) \cdot y \frac{dC}{dy} ,$$

which on integration yields,

$$C = C_{\Phi} \left(\frac{y}{d_T - y}\right)^z \dots (46)$$

in which,

$$z = \frac{V_b}{\beta K \sqrt{\tau_0/\rho}} = \frac{V_b}{\beta K V_*} \dots (47)$$

and  $C_{\Phi}$  is a constant whose value is the concentration at  $y = \frac{d_T}{2}$ .

#### Application to Experimental Data

Equations (41) and (46) describe the air concentration distribution in an open channel. The constants involved can be determined empirically for a given channel, from the observed curves for air concentration.

Firstly the transition depth  $d_T$  and the air concentration  $C_T$  at that depth were determined for a particular discharge and slope from a plot of  $C$  in terms of  $y$ . The point where  $\frac{dC}{dy}$  is maximum is graphically located as in fig. 28(a). The corresponding value of  $d_T$  and  $C_T$  are noted. Using this value of  $C_T$ , the ratio  $\frac{1 - C}{2(1 - C_T)}$  was plotted as a function of  $y$  on probability paper on which a cumulative Gaussian distribution plots as a straight line. Figure 28(b) shows one such plot in the upper region of flow. It is apparent from this that the concentrations possess a cumulative Gaussian distribution.

In the region of flow below  $d_T$  equation (46) indicated that  $C$  is a function of  $\frac{y}{d_T - y}$  and should on a logarithmic plot result in a straight line where slope is equal to the exponent  $z$  and  $C_{\Phi}$  is the value of  $C$  at  $\frac{y}{d_T - y} = 1$ . The logarithmic plot of experimental data as in fig 28(c) shows excellent agreement

with the form of eqn. (-6). In as much as  $C$  approaches infinity as  $y$  approaches  $d_T$ , the experimental data must depart from the curve for larger values of  $\frac{Y}{d_T - y}$  but in this case the data agree with the curve upto  $y/d_T \doteq 0.9$ .

### Relation of Parameters to Flow Conditions

The values of mean air concentration at various slopes for different discharges are shown in fig. 24. It is seen that mean concentration decreases though insignificantly with increasing discharge, and increases considerably with slope. In fact the channel slope, discharge and roughness govern the intensity and scale of turbulence generated. The flow turbulence is created initially at the bed by the wakes and eddies formed by the flow over the roughness elements and the turbulent eddies are then diffused upward into the flow stream. The intensity of turbulence at the transitional surface which is paramount in aeration process, depends upon both the initial generation and the depth of mixture in which it is dissipated. The so called shear velocity may be used as a measure of turbulence generated at bed. Hence the turbulence at the transition surface should vary directly with the shear velocity and inversely with the transition depth  $d_T$ .

Good correlation as shown in fig. 30(a) was obtained between  $\bar{C}$  and  $V_* / d_T^{2/3}$  where  $V_*$  is obtained by

$$V_* = \sqrt{g \cdot d_T \cdot S} \quad \dots \quad (48)$$

Still better correlation was obtained of  $\bar{C}_T$  with  $V_* / d_T^{2/3}$  (Fig. 30(b)).

Figures 31(a) and 31(b) show  $\bar{C}$  and  $\bar{C}_T$  respectively as functions of  $S/q^{1/5}$  where  $S$  is the slope ( $\sin \alpha$ ) and  $q$  is unit discharge. The correlation is seen to be good.

### Influence of Channel Roughness<sup>1</sup>

Observations were taken and similar analysis of data as

above was carried out in case of smooth channel having painted steel surface. It was found in case of smooth channel that mean air concentration correlates with parameter  $V_*/d_T^{4/5}$  and also with parameter  $S/q^{2/3}$ . Since in the parameter  $\frac{V_*}{d_T^m}$ ,  $d_T$  is in denominator and its exponent is smaller in case of rough channels, it is clear that turbulence generated at the bed of rough channel is dissipated to a lesser degree than in case of smooth channel. The exponent  $m$  can be assumed to depend on roughness of channel being smaller for rougher channels.

Comparison of rough and smooth channel air concentration distribution curves in a vertical for a slope of  $45^\circ$  and discharge 0.233 cumec is shown in fig. 29. It is clear that for rough channel the quantity of air entrained is considerably greater, the air is more uniformly mixed and the elevation to which water droplets may be found is considerably greater than that for smooth channel.

#### Effect of Entrained Air on the Flow

Entrained air changes the flow from that of water alone to a mixture of air and water. Experiments were conducted in rough as well as smooth channel to measure the resistance of the boundary to non-aerated flow. The slope was flattened so that for comparable discharges the flow would be non-aerated. The range of discharges was same as in case of aerated flows. The relationships between depth and the discharge and slope for non-aerated flow was obtained by plotting measured depth  $d_n$  as a function of  $\frac{q}{S^{1/2}}$  and found to be as below,

$$q = 50 d_n^{3/2} S^{1/2}, \text{ for rough channel} \quad \dots \quad (49)$$

and  $q = 62 d_n^{3/2} S^{1/2}, \text{ for smooth channel} \quad \dots \quad (50)$

Thus for the range of variables encountered, Chezy's formula describes the data quite well. Assuming a similar equation to be applicable the mean velocity of air-water mixture flowing at a depth  $d_T$  becomes

$$\bar{V} = \text{constt.} \times d_T^{1/2} S^{1/2}$$

Then since  $\bar{d}$  is the depth that represents cross-sectional area of water, the above equation can be written in terms of  $q$  as below,

$$q = \text{constt.} \times \bar{d} \cdot d_T^{1/2} S^{1/2} \quad \dots \quad (51)$$

This relationship verified well when tested by plotting the experimental data for aerated flow for both rough and the smooth channel in the form of  $\bar{d} d_T^{1/2}$  as a function of  $q/S^{1/2}$ . However it was found that the constant maintained the same value as in non-aerated flow i.e. 50 in case of rough channel, and its value increased to 84.5 against 62 of non-aerated flow in case of smooth channel. The reason for this is not apparent but is probably related to a Reynolds number influence for the smooth channel.

The ratios  $\frac{d_u}{d_n}$ ,  $\frac{d_T}{d_n}$ ,  $\frac{\bar{d}}{d_n}$  and  $\frac{\bar{V}}{V_n}$  were also computed using the experimental data for the aerated flow and the computed values of  $d_n$  and  $V_n$  for non-aerated flow. These are shown plotted as a function of the mean concentration  $\bar{C}$  in fig. 32. It is seen that air has little effect on  $d_T$  and  $\bar{d}$  until its percentage exceeds 50%. The velocity of aerated flow remains about the same as that of a corresponding non-aerated flow until the mean concentration is in the neighbourhood of 50%. It then increases rapidly.

It is also seen that  $\bar{d}$  and  $d_T$  change less in comparison with  $d_n$  in case of smooth channel than they do so in case of rough channel. Similarly increase in mean velocity due to

aeration is less for smooth than for rough channel.

### 3.4 STUDIES AT THE CENTRAL WATER AND POWER RESEARCH STATION, POONA<sup>4,7,8</sup>

At the Central Water and Power Research Station, Poona, tests have been carried out for studying the development of air entrainment in open flow in sloping flumes. The slopes tested were 15, 30 and 45, degrees with discharge varied from 0.085 to 0.51 cumec. Most of the experiments were done in a 0.9 m wide cement concrete flume with smooth cement finish and with one side made of perspex to facilitate visual observations. Initial experiments were done in a similar flume 0.3 m wide. Some experiments were repeated with roughened bed also. The observations were made for velocities, water surface and air concentrations.

#### Velocity Observations

Readings were taken with a standard N.P.L. type Pitot static tube. The differential head 'h' which is measured in the Pitot static is connected with the mean velocity head by the relation

$$G^2 h = (1 - C) \frac{v^3}{2g} + \phi C \frac{v^3}{2g} \quad \dots \quad (52)$$

where  $G$  = coefficient of Pitot tube which is slightly less than unity within about half a percent and

$\phi$  = ratio of air to water density

The formula for velocity can therefore be taken as

$$v = G' \sqrt{2gh} \quad \dots \quad (53)$$

where  $G'$  is again a coefficient which for practical purposes may be taken to be unity and the velocities accepted correct to within 2 to 3 percent.

### Water Surface

The water surface was estimated by a point gauge movable with a vernier attachment, and using a simple electrical circuit.

There could clearly be seen the following zones,

A1) a top most zone where there was intermittent spraying, so that this was more in the nature of transport of water sprays inside a current of air,

A2) an intermediate zone near the water surface where the spraying was regular and continuous and,

A3) the continuous water surface below, which contained the normal air entrained masses.

In a slow traverse of the point gage from the top downwards the meter first registered intermittent readings, which were changed to continuously fluctuating +ve readings as zone A2 was reached and steadier values on entering the continuous water surface. The zones A1 and A2 were very small each being about 5% of the water depth.

### Air Concentration Observations

Observations of air concentration at various points of flow were made by using Fifiilar probes. It is an electrical probe consisting of a pair of helically interwound constantan wires, each of 0.3 mm dia and 10 mm length.

The mean air concentration of the flow was determined as

$$\bar{C} = \frac{1}{b_f} \int_0^{b_f} \left\{ \frac{1}{y_u} \int_0^{y_u} C dy \right\} db_f \quad \dots \quad (54)$$

where  $b_f$  = Freadth of channel and  $y_u$  the depth which encompasses 99% of total water discharge.

### Analysis of Data on Smooth and Kough Flumes

The water surface profiles were plotted non-dimensionally



in terms of critical depth 'd<sub>cr</sub>' as shown in fig. 33 and 35 for smooth and rough flumes respectively. These figures also show the mean air concentration  $\bar{C}$  along the flume. It is seen that the dimensionless plot of profiles leads fairly well to a single curve.

The mean air concentration  $\bar{C}$  was also plotted against  $F_R'^2$  defined as

$$F_R'^2 = F_R^2 \cos^2 \alpha \quad \dots \quad (55)$$

where  $F_R^2 = \bar{V}^2 / gR$ ,

$\bar{V}$  = mean velocity and

$\alpha$  = angle of slope of flume.

The plots for smooth and rough flume data are shown in fig. 34 and 36 respectively. A straight line fit has been drawn in both the cases. However there is a considerable scatter.

### 3.5 STUDIES AT INDIAN INSTITUTE OF SCIENCE BANGALORE<sup>24,25,26</sup>

Experiments were conducted in a tilting flume 13.5 m long, 0.45 m wide and 0.375 m deep. The slope of the flume could be adjusted from 0° to nearly 40° w.r.t. horizontal. The experiments were first conducted on smooth aluminium sheet bed and thereafter the bottom was artificially roughened by using sand grains having a mean diameter of 1 mm. The measurement of air concentration was done by an electrical air concentration meter developed in the laboratory. The method consists basically of a measurement of the difference between the conductivity of a mixture of air and water and that of water alone. Measurement of velocity was carried out by a dynamic pressure tapping connected to a manometer. Experimental results were analyzed for two cases viz. (i) developing aerated flow and (ii) fully

developed aerated flow.

### Zones of Flow

According to Rao, Gangadhariah and Seetharamiah<sup>24</sup> flow becomes fully developed turbulent flow when the turbulent boundary layer and the free stream turbulence mixing layer from the free surface meet. The fully developed turbulent flow has been divided into two zones. A lower zone named as wall turbulent zone and an upper zone named Free turbulent zone. The line of demarcation between the two zones has been defined as the locus of points of maximum velocity all along the flow. These divisions will be clear from a perusal of figures 37 and 38. In fact in a more detailed subsequent study<sup>26</sup>, the wall turbulent zone has been further subdivided in accordance with distribution of eddy viscosity into two major regions i.e. inner and outer. Eddy viscosity increases approximately linearly with distance from bed and remains practically constant in the outer region.

### Distribution of Velocity and Air Concentration in Free Turbulent Zone

The theoretical equations which were developed for free turbulent zone based on the analysis of two conflowing streams with a large difference in their densities are,

$$v = \frac{V_m + V_1}{2} - \frac{V_m - V_1}{2} \operatorname{erf} \eta_* \quad \dots \quad (56)$$

for velocity distribution and

$$\frac{1 - C}{1 - C_m} = \frac{1}{2} (1 - \operatorname{erf} \eta_*) \quad \dots \quad (57)$$

for air concentration distribution.

In these equations,

$V_m$  = velocity at line of demarcation

$V_l$  = velocity of air media

and  $\eta_*$  = non-dimensional depth above transition

$$\text{depth} = \frac{y - d_T}{bE}$$

also  $b$  = mixing width measured as twice the distance from transition depth (defined separately for air concentration distribution and velocity distribution) to line of demarcation (Fig. 38),

and  $E$  = a proportionality factor, physically identified as the ratio of eddy diffusivity of momentum to mass.

The theoretical equations (56) and (57) were checked on experimental results and the agreement is found to be very good at all the stations of observations in case of experimental data of rough as well as smooth bed. A few of the plots for illustration are shown in fig. 39.

#### Distribution of Velocity and Air-Concentration in Wall Turbulent Zone

The wall turbulent zone is similar to the fully developed turbulent pipe flow. The eddy viscosity in such cases remains almost constant across its width ( $0.4 \leq \frac{y}{d_m} \leq 1$ ) therefore the concentration distribution, which in turn depends on eddy viscosity also remains constant with in  $0.4 \leq \frac{y}{d_m} \leq 1$ . Extrapolation of theoretical curve given by equation (57) from the free turbulent zone into the wall turbulent zone gives good correlation for smooth boundaries and rough boundaries upto an inclination of  $30^\circ$ . However for rough boundaries for slopes greater than  $30^\circ$ , the correlation is good except near the wall (i.e.  $0 < \frac{y}{d_m} < 0.4$ ).

The velocity distribution in wall turbulent zone for smooth boundaries is expressed by a simple power law relation of the form,

$$\frac{v}{V_m} = \left( \frac{y}{d_m} \right)^{1/j} \dots (58)$$

Where  $j$  is an exponent.

This expression was verified well on experimental data for different discharges and slopes in case of smooth boundaries. Two plots for illustration are shown in fig. 40.

### Detailed Study in Wall Turbulent Zone

More detailed investigations of flow characteristics in wall turbulent zone were made in the hydraulics laboratory of I.I.Sc. Bangalore by K.S.Laxman Rao and T.Gangadhariah<sup>26</sup>. As already indicated this zone was further subdivided into an inner region and an outer region based on the distribution of eddy viscosity which increases approximately linearly as we rise from bed in the inner region and remains practically constant in the outer region.

### Velocity Distribution in Wall Turbulent Zone

The expression developed on theoretical considerations is as below,

$$\begin{aligned} \frac{V_m - v}{V_*} = \frac{2}{3A} \left( \frac{1}{6} \left\{ \frac{1}{0.794} \ln \frac{1}{0.794} - \frac{1}{0.794} \ln \left[ \frac{0.794 - 0.63 \xi + \xi^2}{(0.794 + \xi)^2} \right] \right. \right. \\ \left. \left. - \ln \left[ \frac{\xi^2 + \xi + 1}{(1 + \xi)^2} \right] \right\} + \frac{1}{\sqrt{3}} \left[ \frac{1}{0.794} \tan^{-1} \left( \frac{1}{\sqrt{3}} \right) + \tan^{-1} \left( \frac{-1}{\sqrt{3}} \right) \right. \right. \\ \left. \left. - \frac{1}{0.794} \tan^{-1} \left( \frac{2\xi - 0.794}{0.794 \sqrt{3}} \right) - \tan^{-1} \left( \frac{2\xi + 1}{\sqrt{3}} \right) \right] \right) \dots (59) \end{aligned}$$

This equation gives good agreement with experimental data as is shown in fig. 44.

In this equation,

$$\xi = 1 - \eta \quad \text{where } \eta \text{ is non-dimensional depth given by } \eta = y/d_m \text{ and}$$

A = a constant

Constant A has been empirically correlated with flow characteristics by the following equation,

$$A = 4.48 \left( \frac{d_m}{d_T} \frac{V_*}{V_m} \right)^{1.125} \dots (60)$$

The variation of depth parameter  $d_m/d_T$  with  $V_*/V_m$  also found empirically is given by

$$\frac{V_*}{V_m} = 0.18 \left( \frac{d_m}{d_T} \right)^{1.65} \dots (60A)$$

by knowing  $V_*$  and  $V_m$ ,  $d_m/d_T$  can be found by eqn. (60A) and then A by eqn. (60).

The utility of eqn. (60A) is however not understood by the writer as the very process of determining  $V_*$  and  $V_m$  will be based on a prior determination of velocity and concentration distribution.  $V_m$  and  $d_m$  will be known only from a velocity distribution curve. Further  $V_*$  is computed as  $\sqrt{g d_T \sin \alpha}$ . So this will also require prior knowledge of  $d_T$  which can be determined only after drawing concentration distribution curve. It therefore appears that the constant 'A' does not yield to evaluation by the equations (60) and (60A) in an actual design problem.

#### Distribution of Air Concentration in Wall Turbulent Zone

Theoretical equations developed by Rao and Gangadhariah<sup>26</sup> are ;

For the inner region,

$$C - C_0 = \frac{H \eta_0}{1 - z} \left[ \left( 1 - \frac{\eta}{\eta_0} \right) + \frac{1}{z} \left\{ \left( \frac{\eta}{\eta_0} \right)^2 - 1 \right\} \right] \dots (61)$$

and for the outer region

$$C - C_1 = \frac{H}{z^2} \left[ z (\eta - \eta_1) + 1 - e^{z(\eta - \eta_1)} \right] - \frac{H}{z} \left[ 1 - e^{z(\eta - \eta_1)} \right] \dots (62)$$

In these equations,

$\eta_0$  = non-dimensional depth to outer edge of inner region =  $d_o/d_m$

$C_0$  = air concentration at outer edge of inner region i.e. at  $y = d_o$

and  $C_1$ ,  $\eta_1$  and  $H$  are the values of  $C$ ,  $\eta$  and  $\frac{dC}{dy}$  at  $y = d_m/2$ .

The degree of agreement of theoretical equations (61) and (62) with experimental values is apparent from fig. 43.

The values of  $z$  and  $H$  are correlated with mean air concentration  $\bar{C}_T$  and given below,

$$\bar{C}_T = \frac{1}{1 + 9z} \dots (63)$$

and 
$$\bar{C}_T = \frac{1}{1 + 15.5(-H)^{0.85}} \dots (64)$$

### Position of Inner Zone

Air concentrations in the inner region by eqn.(61) shows an increasing trend and by eqn. (62) in the outer region a decreasing trend towards wall for all values of constants  $z$  and  $H$ . The location of the position of the inner region is found by differentiating eqn. (62) w.r.t.  $\eta$  and putting  $dC/d\eta = 0$  at  $\eta = \eta_0$

The variation of the position of inner zone is shown in fig. 41 which shows a plot of  $d_o/d_T$  v.s.  $\bar{C}_T$  from experimental data,  $d_o$  being normal depth from bed to outer edge of inner region. It is seen that as  $\bar{C}_T$  increases,  $d_o/d_T$  decreases and approximately at about  $\bar{C}_T = 0.20$ , the existence of inner region ceases. Beyond this value of  $\bar{C}_T = 0.20$ , the whole

wall turbulent zone acquires the characteristics of outer region.

### Inception of Air Entrainment<sup>25,4</sup>

Existence of a turbulent free surface is a pre-requisite for the inception of air entrainment. At the inception zone the flow appears to be boiling, with highly agitated ill-defined free surface eddies in the form of projecting masses of flow. These eddies project out of flow and then fall back into the parent medium causing inception to occur. For a water droplet, in the form of an eddy, to project out of the free surface, the kinetic energy it possesses must be greater than the surface tension energy. Based on this concept an air inception parameter  $I$  has been formulated defined by

$$I = (\rho d \bar{V}^2 / \sigma_t) / (V_* d / \nu)^{1/2} \quad \dots \quad (65)$$

which must exceed a certain critical value for inception. This critical value was found to be 56 by experiments. In this eqn.  $\sigma_t$  is surface tension.

An attempt<sup>4</sup> was also made to correlate the Froude number  $F = \sqrt{V/gd}$  with the inception of air entrainment and it was found that  $F = 7.5$  for Veribee weir, 10.6 for Gleumaggie dam and 9.7 for Hickox collected data on Norris and Douglas dams. It appears that this critical value of  $F$  varies to a certain extent with the nature of the boundary which controls turbulence level which in turn affect air inception.

### Locating Point of Inception of Air Entrainment

The concept of air-inception parameter  $I$  is however only of academic interest. It has been found that in all prototype cases the condition of emergence of turbulent boundary

layer on the surface describes necessary as well as sufficient condition for the commencement of air entrainment. In all prototype cases the value of inception parameter at the point of emergence of turbulent boundary layer was calculated at I.I.Sc. to be far greater than the critical value of 56.

To locate therefore the point of inception of air entrainment it would suffice to obtain the point of emergence of turbulent boundary layer on the surface. For this, methods are given by i) Bauer, ii) Campbell and others iii) I.I.Sc.

i) Bauer's Method

For the development of a turbulent boundary layer in wide channels an approximate but practical method has been proposed by Bauer<sup>2</sup>. This method is applicable for spillways and channels provided the flow is accelerating or uniform and if accelerating, then not so rapidly and highly as to cause boundary layer separation. On the results of Bauer's investigations Ven Te Chow<sup>6</sup> has given following formula,

$$\frac{\delta}{x} = \frac{0.024}{(x/\epsilon)^{0.13}} \quad \dots \quad (66)$$

Where  $\delta$  is the thickness of turbulent boundary layer at distance  $x$  from  $O$  in the direction of flow, (Fig. 46) and  $\epsilon$  is the roughness height. The point of inception of air entrainment which is the same as the point of emergence of turbulent boundary layer on the surface can be easily computed by trial finding  $x$  such that  $\delta$  equals depth of flow.

ii) Campbell, Cox and Foyd's Method<sup>3</sup>

For a spillway crest designed for a given head and the flow corresponding to the design head following formula was



proposed by Cambell, Cox and Poyd as a result of their theoretical and experimental investigations,

$$\frac{\delta}{L} = 0.080 \left( \frac{L}{e} \right)^{-0.233} \dots (67)$$

in this equation L is the distance from the upstream edge of the spillway (Fig. 46).

Here again the depth of non-aerated flow will have to be computed by usual methods and L obtained by trial such that  $\delta$  equals depth of flow.

iii) I.I.Sc. Method

The empirical formula which was developed at I.I.Sc. Bangalore by using the results of Sharma<sup>28</sup>; Campbell etc.<sup>3</sup>; Hickox<sup>16</sup>; and Michele and Lovely<sup>22</sup> may be written as,

$$\frac{\delta}{L} = 70 \left( \frac{q}{q_d} \right) \left( \frac{L}{e} \right)^{-0.79} \dots (68)$$

Where  $q_d$  is the design discharge and  $q$  is any discharge per unit width of spillway. This formula can be used in the same manner as Campbell's formula. The advantage however is this that it can be used for discharges other than design discharge also.

Some Characteristics of Uniform Aerated Flows

i) Mean Air Concentration

The local non-aerated Froude number may be defined as

$$F_w = \frac{\bar{V}}{\sqrt{g\bar{d}}} \dots (69)$$

in which  $\bar{V}$  is the mean velocity of aerated flow in a vertical and  $\bar{d}$  is the solid water depth of a given discharge with a mean velocity same as in aerated flow i.e.  $\bar{V}$ .

Using the experimental data of I.T.Sc.<sup>25</sup>, and those of Hall,<sup>15</sup> S.A.F. Laboratory<sup>1,30,31</sup>, and C.W.P.R.S. Poona<sup>7</sup>, an empirical relationship has been developed as follows (Fig. 45),

$$\frac{\bar{C}}{1 - \bar{C}} = \Omega F_w^{3/2} \quad \dots \quad (70)$$

in which  $\Omega$  is a constant depending on the shape and roughness of the channel.

The constant  $\Omega$  is found to vary linearly with Manning's 'n' for a particular shape of the channel (Fig. 42), and the relation between them may be written as

$$\Omega = 1.35 n \quad \dots \quad (71A)$$

for rectangular channels and

$$\Omega = 2.16 n \quad \dots \quad (71P)$$

for trapezoidal channels with side slopes of 1.5:1

ii) Manning's Roughness Coefficient

The presence of air at the solid boundaries reduces frictional effects. Considerable amount of energy will be spent to keep the air bubbles in suspension and to distribute it throughout the flow. The combination of these two factors influences the roughness coefficient.

Assuming the Manning's relation to hold for aerated flow taking transition depth  $d_T$  as the effective depth for computation of velocity

$$V = \frac{1}{n_{aw}} d_T^{2/3} S^{1/2} \quad \dots \quad (72)$$

in case of two-dimensional flow.

Considering that by some means all the air in aerated flow can be removed and that only water can be allowed to flow with air-water

velocity, then according to Rao and Gangadhariah<sup>26</sup>  $d_T$  may be replaced by  $\bar{d}$  and it may be written that,

$$\bar{V} = \frac{1}{n} \bar{d}^{2/3} S^{1/2} \quad \dots \quad (73)$$

In the opinion of the writer however this equation involves a serious error in so much as this equation can not be satisfied without reducing the value of 'n'. This is because the mean velocity of aerated flow increases due to air entrainment above the hypothetical value  $V_n$  of non-aerated flow, computed for the same discharge on the basis of normal value of 'n'. If  $d_n$  is the hypothetical depth of non-aerated flow, then

$d_n = q/V_n$ , and  $V_n = \frac{1}{n} d_n^{2/3} S^{1/2}$ , further since  $\bar{d} = q/\bar{V}$  and  $\bar{V} > V_n$ , therefore  $\bar{d} < d_n$  hence equation (73) can not be satisfied unless n in this eqn. is taken less than the normal value. Nevertheless by comparing this (erroneous) equation (73) with (72) Rao and Gangadhariah deduced,

$$\frac{n_{aw}}{n} = (d_T/\bar{d})^{2/3}$$

and computing values of  $\frac{n_{aw}}{n}$  from this equation using the experimental results of Hall<sup>15</sup>, S.A.F. laboratory<sup>1,30</sup> and I.I.Sc.<sup>26</sup> and plotting it as a function of mean air concentration below transition depth,  $\bar{C}_T$ , obtained that

$$\frac{n_{aw}}{n} = \frac{1}{1 - \bar{C}_T^{1.69}} \quad \dots \quad (74)$$

This shows that roughness coefficient increases with air concentration.

### iii) Relationship between Mean air Concentrations $\bar{C}$ and $\bar{C}_T$

The mean air concentration  $\bar{C}_T$  below transition depth  $d_T$

and mean air concentration of the entire flow have also been correlated by empirical relation,

$$\bar{C}_T = 1.11 \bar{C}^{2.18} \dots (75)$$

## CHAPTER - 4

### DESIGN PROCEDURE

#### 4.0 INTRODUCTION

It is quite apparent from the review of Field and Laboratory studies that the presence of air in water has many effects. As air entrains into the flow, it causes an increase in water volume termed "Bulking". This has undesirable effect on the provision of free board allowances in the design of hydraulic structures. With entrainment of air resistance losses in flow are also affected. Based on the studies carried out in field and laboratories a suitable design procedure is described.

#### 4.1 COMMENCEMENT OF AIR ENTRAINMENT

Air entrainment in a flow commences at a point where turbulent boundary layer emerges on the surface, or in other words where the thickness of turbulent boundary layer equals depth of flow. Non-aerated depths of flow at different sections of the steep chute or spillway can be computed by the usual methods of classical hydraulics. For computation of the turbulent boundary layer along steep chutes or curved surfaces like those of spillways, the following formulae may be used:

##### 1. Ven Te Chow's Formula -

$$\frac{\delta}{x} = \frac{0.024}{(x/\epsilon)^{0.13}} \quad \dots \quad (4.1)$$

##### 2. Campbell, Cox and Foyd's Formula -

$$\frac{\delta}{L} = 0.080 \left( \frac{L}{\epsilon} \right)^{-0.233} \quad \dots \quad (4.2)$$

##### 3. I.I.Sc. Bangalore's Formula -

$$\frac{\delta}{L} = 70 \left( \frac{q}{\alpha_d} \right) \left( \frac{L}{\epsilon} \right)^{-0.79} \quad \dots \quad (4.3)$$

In these equations  $q$  is any discharge,  $q_d$  is the design discharge for spillway surface per unit width,  $e$  is roughness height,  $\delta$  is the thickness of turbulent boundary layer,  $L$  is the distance from the upstream edge of spillway and  $x$  is the distance measured parallel to chute channel or spillway slope from the water surface to the total energy line (Fig.46).

#### 4.2 MEAN AIR CONCENTRATION

For estimating mean air concentration in the flow, formulae given by Hall, U.S. Army or I.I.Sc. Bangalore may be used.

##### 1. Hall's Formula -

According to Hall ratio of volume of air to that of water is given by

$$\frac{\bar{C}}{1 - \bar{C}} = K \frac{V^2}{9R_c} \quad \dots \quad (4.4)$$

Where  $V$  is the mean velocity of air water flow and  $R_c$  is the hydraulic radius of solid water flow alone of a given discharge with a velocity equal to that of air water flow i.e.  $V$  and  $\bar{C}$  is the mean air concentration. Also  $K$  is a constant whose value under average conditions may be taken as 0.005.

##### 2. U.S. Army's Formula<sup>32</sup> -

The U.S. Army Waterways Experiment Station Vicksburg, have analysed on a digital computer smooth channel data of S.A.F. Laboratory and rough channel data of S.A.E. Laboratory in combination with selected Kittitas chute results, selected on the basis of observations with depth of flow less than 1/5th width, which tentatively defines a wide channel where flow can be assumed to be two-dimensional in character and have given the following formulae for mean air concentration  $\bar{C}$  for a discharge  $q$  in

cumec per metre on slope  $S$  for cases of fully developed aerated flows,

$$\bar{C} = 0.38 \log_{10} \left( \frac{S}{q^{2/3}} \right) + 0.51 \quad \dots \quad (4.5)$$

- for smooth channel

$$\bar{C} = 0.743 \log_{10} \left( \frac{S}{q^{1/5}} \right) + 0.721 \quad \dots \quad (4.6)$$

- for rough channel

### 3. I.I.Sc. Bangalore's Formula -

Another empirical formula which was developed at I.I.Sc. Bangalore may be written as,

$$\frac{\bar{C}}{1 - \bar{C}} = \Omega F_w^{3/2} \quad \dots \quad (4.7)$$

Where constant  $\Omega$  is related to Mannings 'n' for a particular shape of the channel,

$$\Omega = 1.35 n \text{ for a rectangular channel}$$

and  $\Omega = 2.16 n$  for trapezoidal channels of 1.5:1 side slope

and  $F_w$  is the non-aerated Froude number given by

$$F_w = \bar{V} / \sqrt{g\bar{d}} \quad \dots \quad (4.8)$$

in which  $\bar{V}$  is mean velocity of flow and  $\bar{d}$  is mean solid water depth.

### 4.3 BULKAGE DEPTH AND HEIGHT OF GUIDE WALLS

The bulkage depth factor may be defined as the ratio of the excess depth due to air entrainment over the calculated mean solid water depth of flow,

$$F = \frac{d_u - \bar{d}}{\bar{d}} \quad \dots \quad (4.9)$$

In terms of air concentration bulkage depth factor may be written as

$$F = \bar{C} / (1 - \bar{C}) \quad (4.10)$$

Once  $\bar{C}$  is known by any of the formulae given in para 4.2, P and thereby  $d_u$  i.e. the upper limit of flow can be computed by these equations. The height of guide walls of a chute spillway is then equal to the depth  $d_u$  plus a free board.

## 2. S.A.F. Procedure

Another simple and direct method of determining the upper limit of flow depth  $d_u$  in two-dimensional uniform aerated flows is the use of curves in fig. 32 given by Anderson of S.A.F. laboratory. Depth ' $d_n$ ' of non-aerated flow can be computed by the usual Manning's formula and then the ratio  $d_u/d_n$  read directly from the curves corresponding to rough or smooth channel as the case may be for the already determined value of mean air concentration  $\bar{C}$ .

## 3. Halls' Method

For the general case of developing aerated flow however, it appears that the best would be to use the method developed on the basis of Hall's theory which is outlined below:

Let the channel have an inclination  $\theta$  degree w.r.t. horizontal and let  $A_c$ ,  $R_c$ ,  $Y_c$  denote respectively the area, hydraulic radius, and depth of solid water flow of a given discharge with the same mean velocity  $V$  as in the actual air-water mixture flow. Let subscripts 1 and 2 refer respectively to sections 1-1 and 2-2 distance  $L$  apart.

Applying Bernoulli's theorem

$$\frac{n_c^2 Q^2}{A_c^3 (R_c)^{4/3}} = \left( \frac{Y_{c1} - Y_{c2}}{L} \right) \cos \theta + \sin \theta + \frac{\alpha_a}{2gI} (V_1^2 - V_2^2) \dots (4.11)$$

In this equation  $\alpha_a$  is the energy correction coefficient and  $n_c$  is given by,



$$n_c = n (R_c/R)^{2/3} \quad \dots (4.12)$$

where  $R$  is the hydraulic radius of air-water mixture flow and 'n' is the normal value of Manning's coefficient.

In using the above equation (4.11), a value of  $Y_{c2}$  is first assumed and corresponding value of  $V_2$  is calculated by dividing  $Q$  by the area of cross-section  $A_{c2}$  at depth  $Y_{c2}$ .  $R_c$  is mean of  $R_{c1}$  and  $R_{c2}$ . Then  $\bar{C}$  can be computed by using Hall's formula or better by using I.I.Sc. Bangalore's formula. Once  $\bar{C}$  is known, actual area  $A = A_c / (1 - \bar{C})$  and thereby actual hydraulic radius 'R' of air water mixture flow can be computed. This would enable determination of  $n_c$  by equation (4.12). Now all the quantities involved in equation (4.11) are known and if correct value of  $Y_{c2}$  is assumed the two sides must balance otherwise another value of  $Y_{c2}$  must be tried. The step by step computations in this manner have to be carried out starting from the section of commencement of air entrainment.

## CHAPTER - 5

### CONCLUSIONS

#### 5.0 INTRODUCTION

High velocity open channel flow differs from the normal flow of water in open channels dealt in classical hydraulics in as much as another fluid <sup>viz.</sup> ~~like~~ air from the surrounding atmosphere gets insufflated into and mixed with the flow. The water becomes white and the surface of flow becomes rough and ill defined. The insufflation of air causes not only bulking of flow but it also affects the velocity of flow and the resistance losses in the channel. The quantity of air entrained depends on the degree of turbulence which is generated at the channel boundary. Various laboratory and field studies have been conducted in the past on the initiation and development of air entrainment in high velocity flows, the quantity of air entrained and its distribution, the factors which affect air entrainment and the effects of air entrainment on flow properties. These studies have been described in the preceding chapters and the conclusions drawn therefrom are described briefly in this chapter.

#### 5.1 MECHANISM OF THE PHENOMENON

Air entrainment is a continuous process of droplets of water projecting from the liquid into the air above and air bubbles penetrating into the liquid mass. Transverse component of turbulent velocity fluctuations, when become sufficiently strong near the air water interface cause clumps of water to break through the surface into the air and then fall back by gravity into the flowing stream. These clumps of water break into a heterogeneous spray of globules and droplets which engulf a certain amount of air leading to

insufflation of air into the stream. Air being very light as compared to water remains in a statistical equilibrium between the forces of buoyancy on one hand which tend to separate air bubbles from water and forces of turbulent transfer on the other hand which tend to distribute air bubbles in flowing water.

## 5.2 INCEPTION OF AIR ENTRAINMENT

Existence of a turbulent free surface is a pre-requisite for the inception of air entrainment. Since turbulence is generated at the boundary it follows that turbulent boundary layer must emerge on surface before air entrainment can commence. This is also corroborated by the fact that distance  $L$  from the inlet end upto the commencing point of air entrainment increases as the unit discharge on a spillway increases and that immediately prior to the point of commencement of air entrainment the surface of flow shows characteristic roughening. Based on the concept that the eddies in the form of droplets of water will project out of free surface to cause inception of air an 'Inception Parameter' was formulated at I.I.Sc. Bangalore whose value must exceed a certain critical value. This was however found to be only of academic interest as in all prototype cases, some preliminary calculations done by investigators at I.I.Sc. Bangalore have shown that at the section at which turbulent boundary layer emerges, the value of 'Inception Parameter' is considerably greater than the critical value. Hence it can be concluded that the emergence of turbulent boundary layer on the surface of flow describes necessary as well as sufficient condition for inception of air entrainment.

### 5.3 DISTRIBUTION OF VELOCITY IN AERATED FLOW

This was studied by Viparelli at Naples and Rao and others at I.I.Sc. Bangalore. For this purpose the flow has been divided into two zones viz, a lower region and an upper region. The velocity first increases as we rise from bed and then decreases, the maximum value occurring at the point which defines the demarcation between the two regions (Fig. 38). According to Viparelli the flow in layers near the bottom is governed by the usual logarithmic law of velocity distribution. This can be expected otherwise also as in these layers air concentration is comparatively small and the flow is predominantly that of water. At I.I.Sc. Bangalore a simple power law relation for smooth channels was given first (eqn. 58) and later on a complicated expression (eqn. 59) was evolved as a result of more detailed subsequent investigations.

For flow in upper regions velocity distribution is well described by the expression developed at I.I.Sc. Bangalore (eqn. 56).

### 5.4 DISTRIBUTION OF AIR CONCENTRATION

A typical air concentration distribution profile is shown in fig. 29. The concentration of air increases gradually from the bed, more rapidly in the central portion and then more slowly in the upper region, apparently asymptotically approaching the limit of 100%. Straub and Anderson divided the flow into two regions viz, an upper and a lower region. The upper region consists primarily of independent droplets and larger agglomerations of water that move independently of the stream proper and in the lower region discrete air bubbles are suspended in the stream and are distributed by the mechanism of turbulence.

The distribution of water air agglomerate and droplets is adequately described by the Gaussian cumulative probability equation (eqn. 41). Equation 46 was developed on the basis of turbulent mixing for describing the distribution of air concentrations in the lower region.

At I.I.Sc. Bangalore also the flow has been divided into two zones viz., a wall turbulent zone and a free turbulent zone with the point of maximum velocity in a vertical being the demarcation. The wall turbulent zone is further subdivided into an inner region near the bottom and an upper region based on the distribution of eddy viscosity. The expressions for distribution of air concentration in different zones are given by equations 57, 61 and 62.

## 5.5 FACTORS AFFECTING AIR ENTRAINMENT

Various factors which affect air entrainment are

- i) Discharge
- ii) Slope of channel
- iii) Velocity of flow
- iv) Roughness of boundary.
- v) Side walls

### 1. Effect of Discharge

As can be seen from fig. 24 the mean air concentration for a given channel slope decreases with increasing discharge. However the effect is not very prominent in case of flow in rough channels. It is more significant in case of flow in smooth channels. From the studies conducted at S.A.F. laboratory we know that air concentration increases with the parameter  $S/q^{1/5}$  in case of rough and  $S/q^{2/3}$  in case of smooth channels. The

exponents of unit discharge  $q$  being  $1/5$  in rough and  $2/3$  in smooth channel quantify the relative effects of discharge.

## 2. Effect of Slope

Air entrainment increases with the slope and the effect is much more significant than that of discharge as can be easily inferred from fig. 24. In fact mean air concentration varies directly as the logarithm of slope of the channel (Eqn. 4.5 and 4.6). It follows from this that variation would be less prominent at steeper slopes.

## 3. Effect of Velocity of Flow

In case of uniform flow the discharge and slope automatically fix the velocity. However for developing aerated flow or in other words in case of varied flow effect of velocity must be known independently. From Hall's formula (Eqn. 4.4) and that developed at I.I.Sc. Bangalore (Eqn. 4.7), we find that air concentration increases with Froude number which increases with velocity of flow. Thus for a given discharge mean air concentration increases with velocity.

## 4. Effect of Roughness of Channel Boundary

An increase in roughness results in greater air concentration and more uniform mixing of air, obviously due to creation of a more intense turbulence and greater velocity fluctuations. Figure 29 shows clearly the effect of roughness on air concentration.

## 5. Effect of Side Walls

Figures 12 and 25 show the air concentration distribution across sections of fully developed aerated flow. The air

concentration contours are considerably higher near the side walls than in the central region of the flow. The aeration is initiated earlier at the water surface near side walls than in the central region.

## 5.6 EFFECTS OF ENTRAINED AIR ON THE FLOW

The entrained air has the effect of changing the flow from one of water alone to that of a mixture of air and water which besides increasing the bulk depth affects the velocity of flow and resistance losses also.

### 1. Effect on Mean Velocity

Hall very emphatically said that the velocity of flow increases due to air entrainment. This was later on conclusively shown to be so by Straub and Anderson when they compared in a plot covering a wide range of discharges and slopes, the ratios  $\bar{V}/V_n$  (of actual observed mean velocity of air entrained flow and the hypothetical mean velocity of non-aerated flow) v.s. the mean air concentration  $\bar{C}$  (Fig. 32). It is obvious from this plot that the mean velocity of an air entrained flow is greater than that of a corresponding non-aerated flow by an amount that increases with the air concentration.

### 2. Effect on Manning's Roughness Coefficient

The presence of air at the solid boundaries reduces frictional effects, however energy is spent in keeping the air bubbles in suspension in the flow. The combination of these two factors influences the roughness coefficient. The views of different investigators are summarized below:

(i) Hall considers that air in and above water causes no additional loss in energy. The reduction in specific gravity due

to air entrainment compensates for the added area and roughness coefficient 'n' remains constant when total depth of flow is considered effective for computation of velocity.

(ii) Jevdjevich and Levin contend that there are two opposite influences viz the effect of super-rapid flow which acts so as to increase 'n' and the effect of entrained air which acts so as to reduce the value of 'n'. At low Froude numbers the first influence dominates and <sup>at</sup> higher values of Froude number the second influence dominates.

(iii) Viparelli in his investigations at Naples calculated Mannings 'n' considering only the flow in layers near bottom and found that 'n' remains more or less same. He obtained similar results on analysing Gizeldon chute data.

(iv) Straub and Anderson at S.A.F. laboratory have shown the aerated flow velocities to be higher than corresponding velocities for the same discharges computed on the basis of the usual non-aerated flow formula. Chezy's formula was found to describe the relationship of mean velocity and depth of flow in case of non-aerated as well aerated flows for the range of discharges and slopes investigated. The value of Chezy's constant was found to be same in both types of flow in case of rough channel and higher in aerated flow in case of smooth channel. Chezy's constant  $C_z$  is related to Mannings  $n$  by the relationship,

$$C_z = \frac{1}{n} R^{1/6}$$

Now  $R$  increases in aerated flow but the effect it causes on the value of  $C_z$  is insignificant as its influence is reflected in 1/6th power. Hence in rough channel 'n' should only increase insignificantly to maintain same value of  $C_z$ . In smooth channels however since  $C_z$  increases significantly for aerated flows



hence  $n$  should decrease to a certain extent.

(v) At I.I.Sc. Bangalore it has been shown that value of ' $n$ ' increases in aerated flows as is apparent from eqn. 74. However as already discussed by the writer this equation seems to have been developed somewhat erroneously.

Fearing the above discussion in mind the writer is inclined to suggest that till further researches establish definite relationship for the effect of aeration on the value of ' $n$ ' it may be assumed to maintain the same value in aerated flows as in case of normal non-aerated flow.

## APPENDIX - I

### REFERENCES

1. Anderson, A.G., "Influence of channel roughness on aeration of high velocity, open channel flow", - Proc. IAHR, 1965, vol I.
2. Pauer, W.J., "Turbulent boundary layer on steep slopes", Trans. A.S.C.E. vol 119, 1954.
3. Campbell, F.L., R.G. Cox and M.P. Eoyd, "Boundary layer development and spillway energy losses", Hyd. dn. ASCE, May 1965.
4. C.F.I. and P., Annual Review of Fundamental and Basic Research, 1959-63.
5. C.F.I. and P., Technical Report No. 8, November 1970.
6. Chow, Ven Te "Open channel Hydraulics", International students' edition, page 198.
7. C.W.P.R.S., Poona, "Annual Report (Tech.)" 1952-56, 1958, 1959.
8. C.W.P.R.S., Poona, "Review on Air Entrainment in High Velocity Flow", January 1965.
9. Corwin, T.J.Jr., discussion of "Open Channel Flow at High Velocities", by L.S. Hall, Trans. A.S.C.E. vol 108, 1943.
10. DeLapp, W., discussion of "Open channel Flow at High Velocities", by L.S.Hall, Trans. A.S.C.E. Vol 108, 1943.
11. Douma, J.H., discussion of "Open Channel Flow at High Velocities", by L.S.Hall, Trans. A.S.C.E. vol 108, 1943.
12. Ehrenberger, E., "Flow of water in steep chutes with special reference to self aeration" Accession No. 4943, C.F.P.C. Library.
13. Gumensky, D.F., "Air entrainment in fast water affects design of training walls and stilling basins", Civil Engg. (A.S.C.E.) vol 19, No. 12, Dec. 1949.
14. Halbronn, G., R. Durand, and G.Cohen De Lara, "Air entrainment in steeply sloping flumes" Proc. IAHR 1953.
15. Hall, L.S., "Entrainment of air in flowing water", (symposium); "Open channel flow at high velocities", Trans. A.S.C.E. vol 108, 1943.
16. Hickox, G.H., "Air entrainment on spillway faces", Civil Engg. (A.S.C.E.) vol 15, No.12, Dec. 1945.

17. Hino, T., "On the mechanism of self aerated flow on steep slope channels, Application of the statistical theory of turbulence", Proc. I.A.H.R., 1961.
18. Jevdjevich, V. and L. Levin, "Entrainment of air in flowing water and technical problems connected with it", Proc. I.A.H.R., 1953.
19. Knapp, R.T., discussion of "Open channel flow at high velocities", by L.S.Hall, Trans. A.S.C.E. vol 108, 1943.
20. Lane, E.W., "Recent studies on flow conditions in steep chutes", Eng. News Record, January 2, 1963.
21. Mc.Connaughy, D.C., discussion of "Open channel flow at high velocities", by L.S. Hall, Trans. A.S.C.E. vol. 108, 1943.
22. Michels, V., and M. Lovely, "Some prototype observations of air entrained flow", Proc. I.A.H.R. 1953.
23. Pavel, D., "Flow of water mixed with air in channels and on spillways", Hyd. Proc., Budapest, No.2, 1951.
24. Rao, N.S.L., K.Seetharamiah and T.Gangadhariah "Characteristics of self aerated flows", Hyd. dn. A.S.C.E., Feb. 1970.
25. Rao N.S.L., K. Seetharamiah and T. Gangadhariah "Inception and entrainment in self aerated flows", Hyd. dn. A.S.C.E., July 1970.
26. Rao, N.S.L. and T.Gangadhariah, "Self aerated flow characteristics in wall region", Hyd. dn. A.S.C.E., Sept. 1971.
27. Seetharamiah, K. and T. Gangadhariah, "Air entrainment at high velocities in chutes, nozzles, expansions etc." Proc: symposium on High velocity flows, I.I.Sc. Bangalore 1967.
28. Sharma, Y.C., "Development of Boundary Layer Characteristics on Curved Walls with reference to Spillways", Thesis for M.E. at I.I.Sc. Bangalore 1968.
29. Stevens, J.C., discussion of "Open channel flow at high velocities", by L.S.Hall, Trans. A.S.C.E. vol 108, 1943.
30. Straub, L.G. and A.G. Anderson, "Experiments on self aerated flows in open channels", Hyd. dn. A.S.C.E. Dec. 1958, also in Trans. A.S.C.E. 1960.
31. Straub, L.G. and O.Lamb, "Experimental Studies of air entrainment in open channel flow" Proc. I.A.H.R., 1953.

32. Task Committee on Air Entrainment in Open Channels, "Aerated flow in open channels", Hyd. dn. A.S.C.E., May 1961.
33. Viparelli, M., "The flow in a flume with 1:1 slope", Proc. I.A.H.R., 1953.
34. Viparelli, M., "Fast water flow in steep channels", Trans. I.A.H.R. 1957 vol II.

## APPENDIX - II

### NOTATION

Symbols have generally been defined where used. A list of symbols used more commonly is, however, given below:

- A = Area of flow cross-section
- $A_c$  = Area of non-aerated flow of a given discharge with the same velocity as in aerated flow
- B = Fulkage depth factor
- b = Mixing width for air concentration distribution and velocity distribution
- $b_f$  = Width of flume
- C = Air concentration i.e. volume of air per unit volume of air-water mixture
- $\bar{C}$  = Mean air concentration in a vertical section
- $C_o$  = 'C' at  $y = d_o$
- $C_l$  = 'C' at  $y = d_m/2$
- $C_T$  = 'C' at  $y = d_T$
- $C_{\frac{T}{2}}$  = 'C' at  $y = d_T/2$
- $\bar{C}_T$  = Mean air concentration in region between  $y = 0$  and  $y = d_T$
- $C_m$  = 'C' at  $y = d_m$
- $d, Y$  = Depth of flow at a point measured normal to bed
- $\bar{d}, Y_c$  = Depth of non-aerated flow of a given discharge with the same velocity as in aerated flow
- $d_{cr}$  = Critical depth
- $d_m$  = Value of 'y' at the demarcation between wall turbulent zone and free turbulent zone
- $d_n$  = Depth in non-air entrained flow of a given discharge
- $d_o$  = Value of 'y' at the outer edge of inner wall region
- $d_T$  = Transition depth
- $d_u$  = Upper limit of flow or value of 'y' where  $C = 0.99$
- E = A proportionality factor, physically identified as the ratio of eddy diffusivity of momentum to mass

- e = Base of Napierian logarithms
- F =  $V/\sqrt{gd}$  = Froude number
- $F_R$  =  $V/\sqrt{gR}$  = Froude number with hydraulic radius used as a characteristic length
- $F_w$  =  $\bar{V}/\sqrt{gd}$  = Non aerated Froude number
- g = Acceleration due to gravity
- h = Head on the tip of Pitot tube
- I = Inception parameter
- K = Constant
- L = Distance along profile from upstream edge of a spillway
- n = Manning's roughness coefficient
- $P_c$  = Perimeter of computed non-aerated flow section  $A_c$
- $p_w$  = Water factor i.e. volume of water per unit volume of air-water mixture =  $1 - C$
- Q = Discharge
- q = Unit discharge i.e. discharge per unit width
- $q_d$  = Unit design discharge for spillway profile
- $q_s(y)$  = Unit discharge in region above y
- R = Hydraulic radius
- $R_c$  = Hydraulic radius of computed non-aerated flow section  $A_c$
- S = Slope of channel ( $\sin \alpha$ ) in uniform flow, friction slope
- $u_q$  = Water discharge rate per unit area of air-water mixture section
- v = Velocity of flow at any point (Local value)
- $V, \bar{V}$  = Mean velocity in a vertical section
- $V_1$  = Undisturbed velocity of air media
- $V_b$  = Rising velocity of air bubbles
- $V_m$  = Velocity at  $y = d_m$
- $V_n$  = Velocity in non-air entrained flow of a given discharge
- $V_*$  =  $\sqrt{\tau_0/\rho}$  =  $\sqrt{g d_T S}$  = shear velocity
- x = Distance measured in flow direction along the centre line of flume from inlet

- $y$  = Distance of any point in flow from channel bed  
 $y'$  =  $y - d_T$  = height above transition depth  
 $\alpha$  = inclination of channel bed w.r.t. horizontal  
 $\alpha_a$  = energy correction factor  
 $\gamma_w$  = weight of water per unit volume  
 $\delta$  = Thickness of boundary layer  
 $\epsilon$  = mean roughness height  
 $\eta$  =  $y/d_m$  = non-dimensional depth  
 $\eta'$  =  $(y - d_T)/b$  = non-dimensional depth  
 $\eta_*$  =  $\eta'/E$  = non-dimensional depth  
 $\theta$  = Inclination of channel bed w.r.t. horizontal  
 $K$  = Von Karman's universal constant for velocity distribution  
 $\nu$  = Kinematic viscosity of water  
 $\xi$  =  $1 - \eta$  = non-dimensional depth  
 $\rho$  = Mass density of water  
 $\sigma$  = Standard deviation for air distribution  
 $\sigma_t$  = Surface tension  
 $\tau_0$  = Shear stress at the boundary of flow  
 $\Omega$  = Constant depending on shape and roughness of channel  
 $\text{erf } \eta_* = \frac{2}{\sqrt{\pi}} \int_0^{\eta_*} e^{-\eta_*^2} d\eta_*$

U N I T S

All dimensions are in Metric Units. All the figures and formulae quoted in this dissertation have been converted accordingly.

## APPENDIX - III

### FIGURES

Figures given in this dissertation are after the References indicated against each in the table given below. All the figures have been converted into metric units and symbols have been changed at some places to correspond to the symbols used in the text of dissertation.

Figure No.	Serial No. of Reference in Appendix - I
1,3,4	22
2,5,6,7	15
8,9,10,11,16	18
12,13,14,15	14
17,18,19,20	33
21,22,23	34
25,26,27	31
24,28,30,31	30
29,32	1
33,34,35,36	8
37,38,39,40	24
42	25
41,43,44	26
45	5



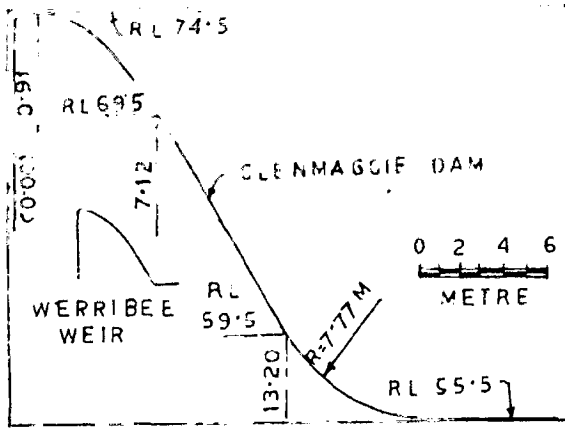


FIG 1 PROFILES OF GLENMAGGIE DAM AND WERRIBEE DIVERS ON WEIR

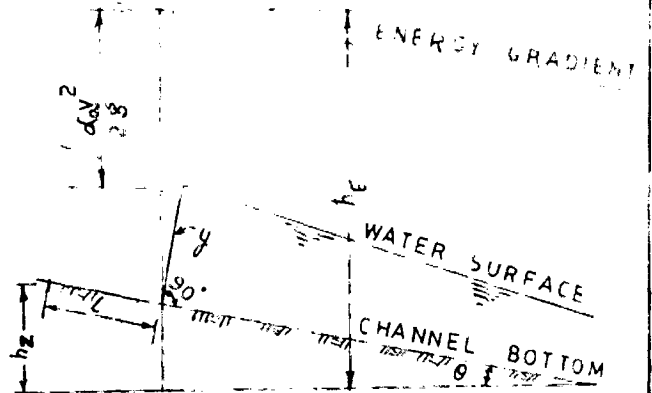


FIG 2 DEFINITION SKETCH FOR ENERGY EQUATION

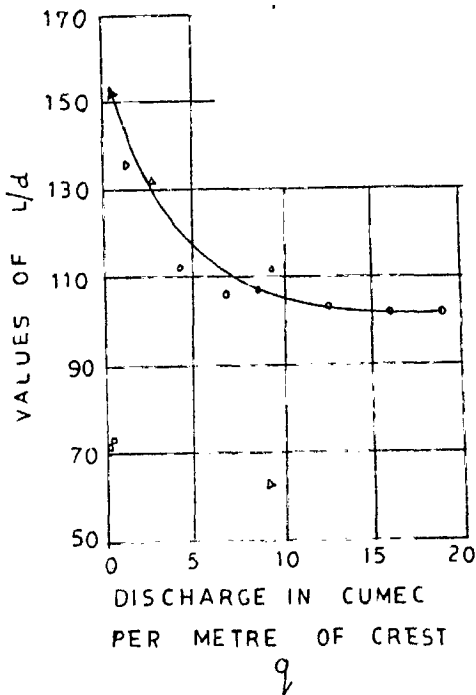


FIG 3  $L/d$  VERSUS DISCHARGE

LEGEND

- HICKOX MODEL DATA
- △ GLENMAGGIE DAM PROTOTYPE
- WERRIBEE DIVERSION WIER

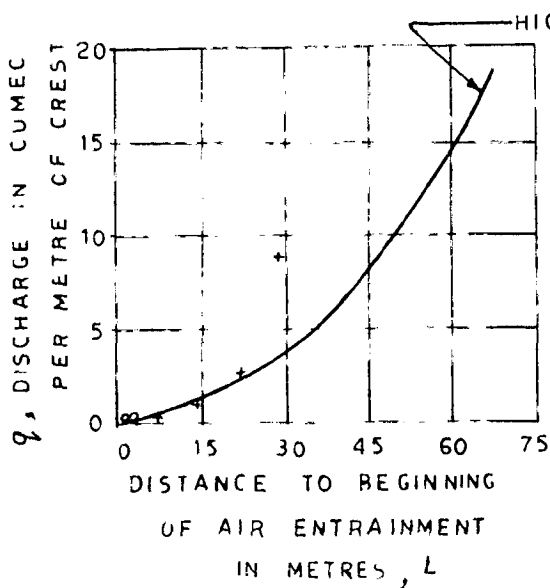


FIG 4 DISTANCE TO BEGINNING OF AIR ENTRAINMENT VERSUS DISCHARGE

LEGEND

- + GLENMAGGIE DAM
- o WERRIBEE DIVERSION WIER

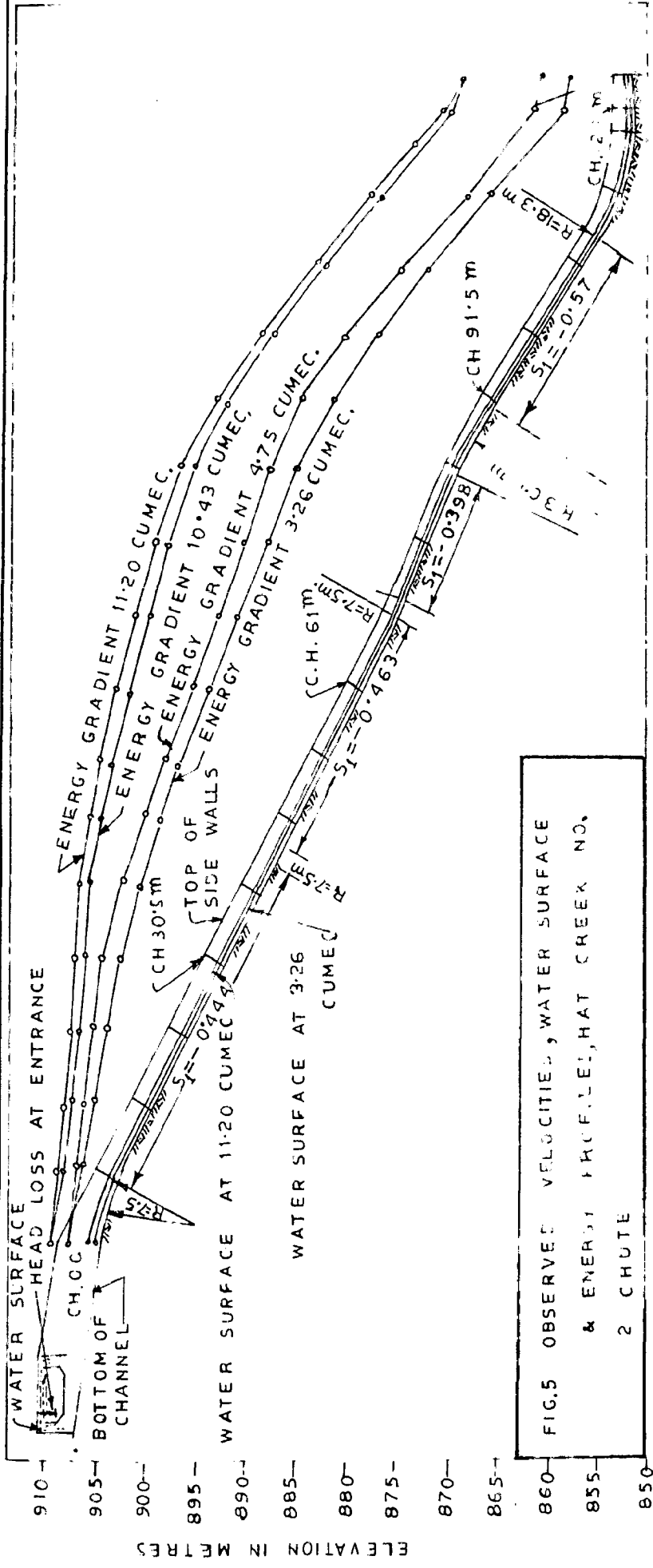


FIG. 5 OBSERVED VELOCITIES, WATER SURFACE & ENERGY PROFILES, HAT CREEK NO. 2 CHUTE

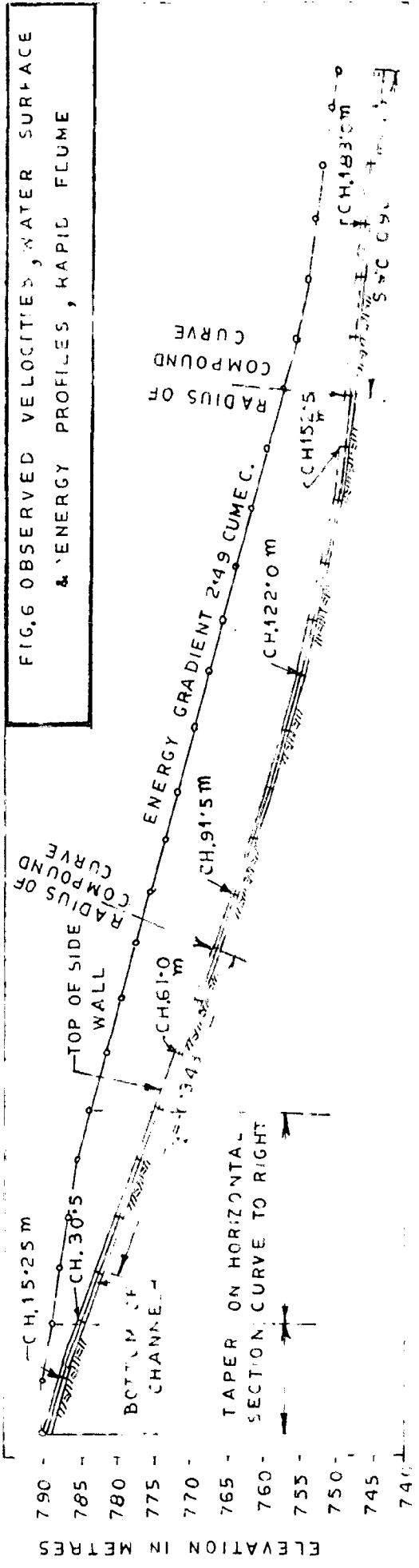


FIG. 6 OBSERVED VELOCITIES, WATER SURFACE & ENERGY PROFILES, RAPID FLUME

ELEVATION IN METRES

ELEVATION IN METRES

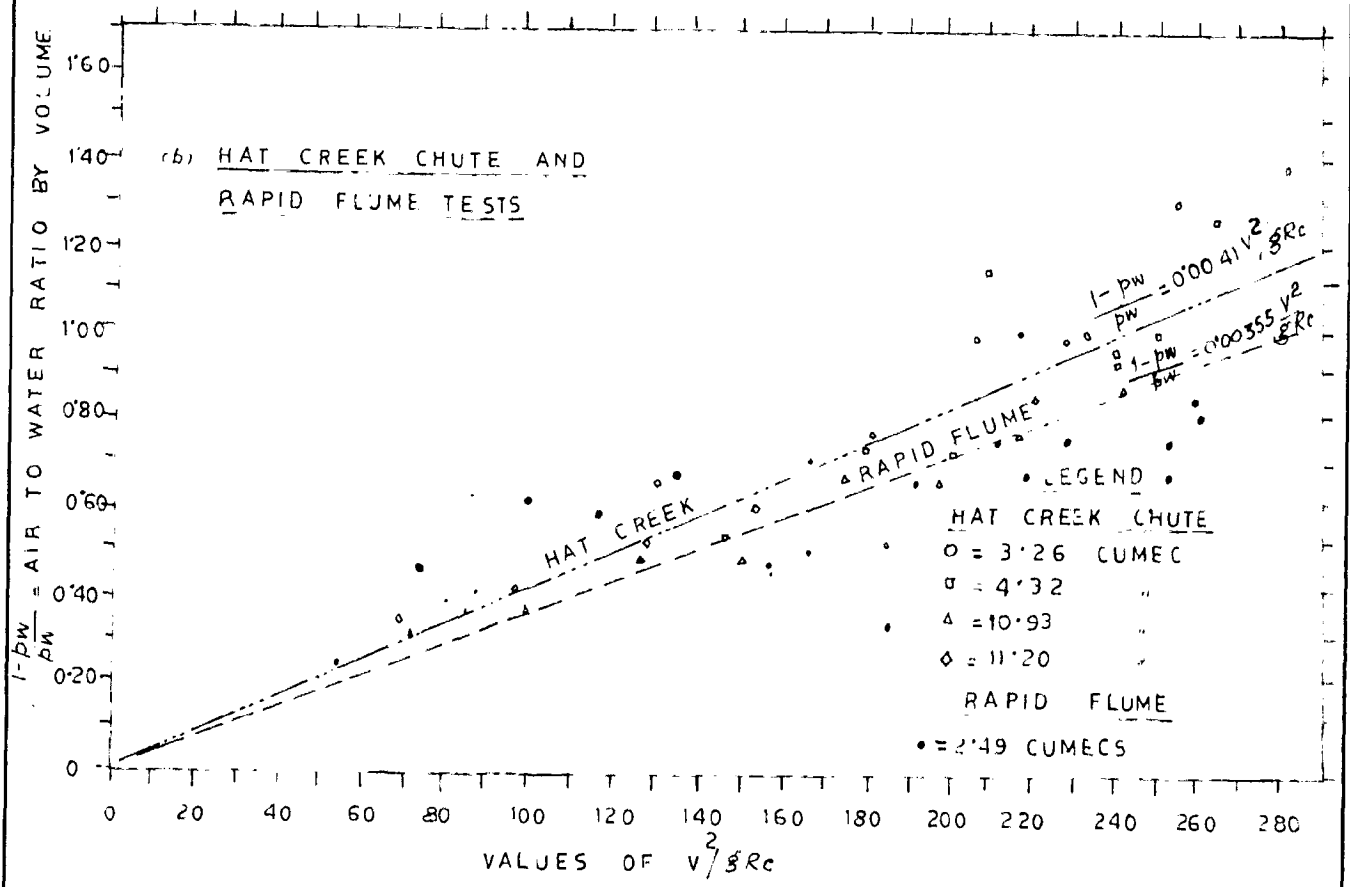
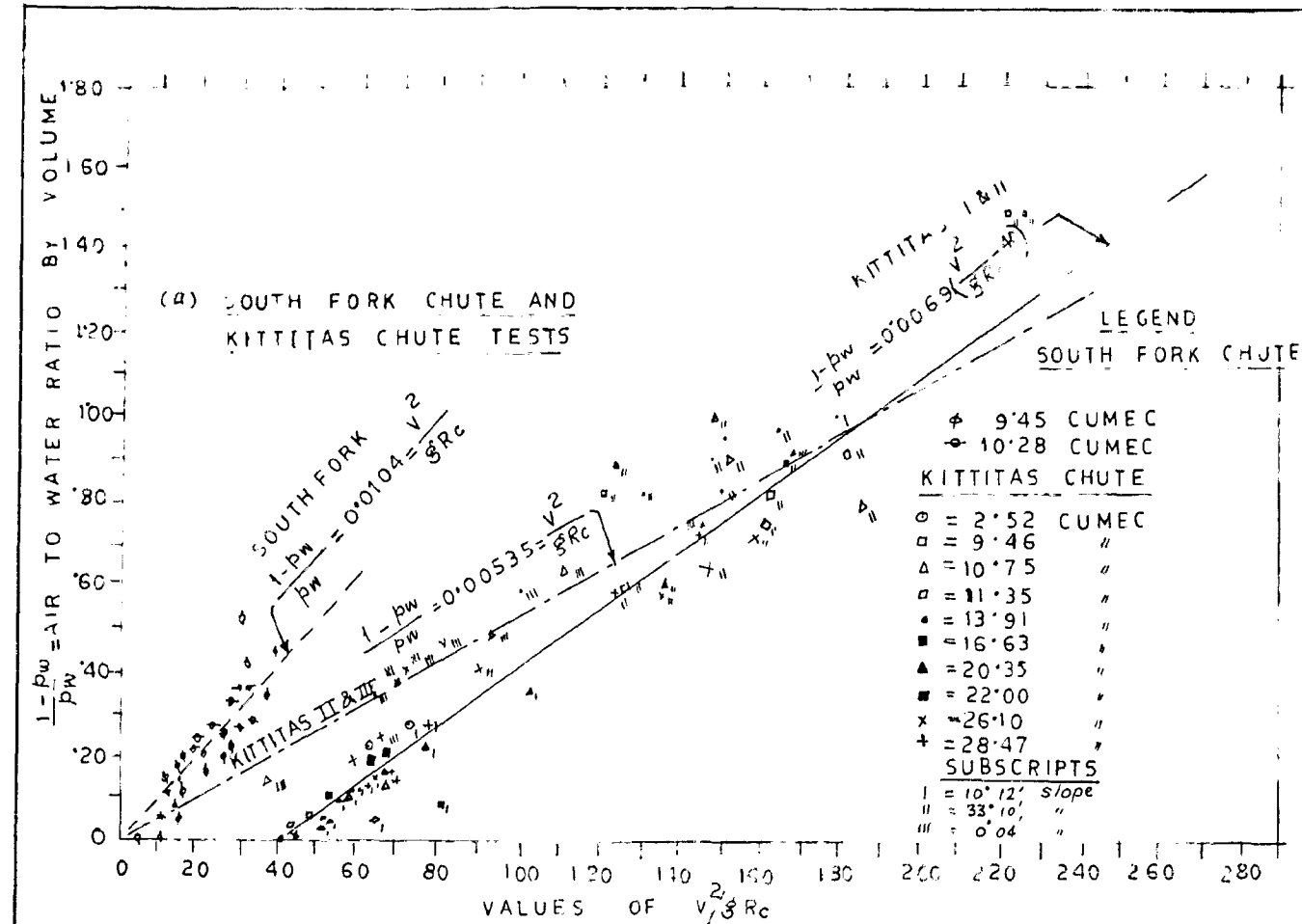


FIG. 7. RELATION OF AIR-WATER RATIO TO  $\frac{V^2}{gRc}$

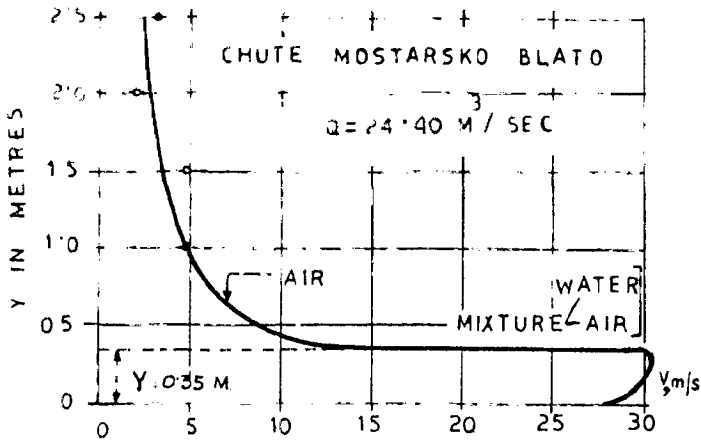


FIG. 8 VELOCITY DISTRIBUTION IN THE STEEP CHUTE CHANNEL "MOSTARSKO BLATO" FOR AIR WATER MIXTURE AND FOR AIR ABOVE IT

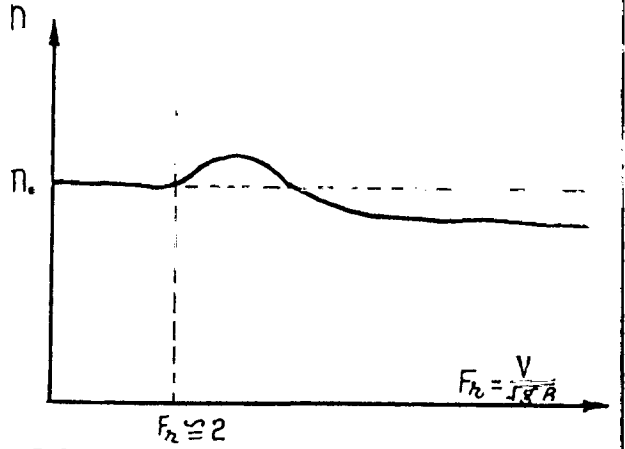


FIG. 9 VARIATION OF THE RESISTANCE COEFFICIENT  $\eta$  TO THE NUMBER  $Fr = \frac{V}{\sqrt{gR}}$

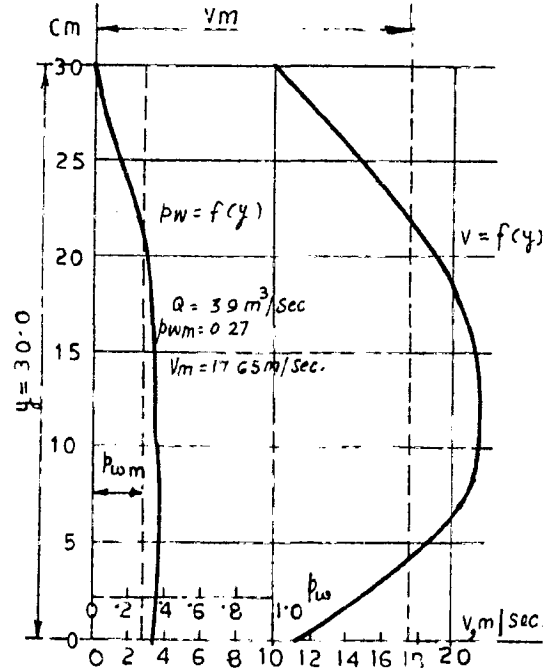
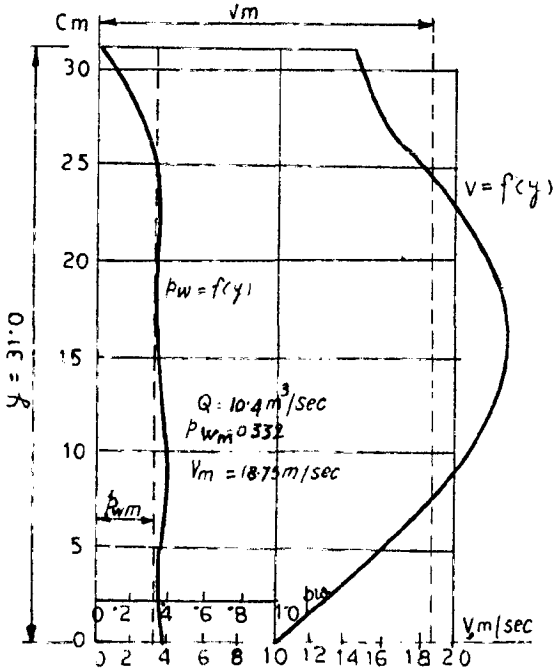


FIG 10

$\alpha_a = \frac{\sum p_w V^3 \Delta y}{P_w V_m^3 Y} = \frac{74739}{0.311 \cdot 6592.31} = 1.118$  VELOCITY AND WATER FACTOR DISTRIBUTION AT MOSTARSKO BLATO CHUTE CHANNEL

$\alpha_a = \frac{\sum p_w V^3 \Delta y}{P_w V_m^3 Y} = \frac{55380}{0.27 \cdot 5498.30} = 1.24$

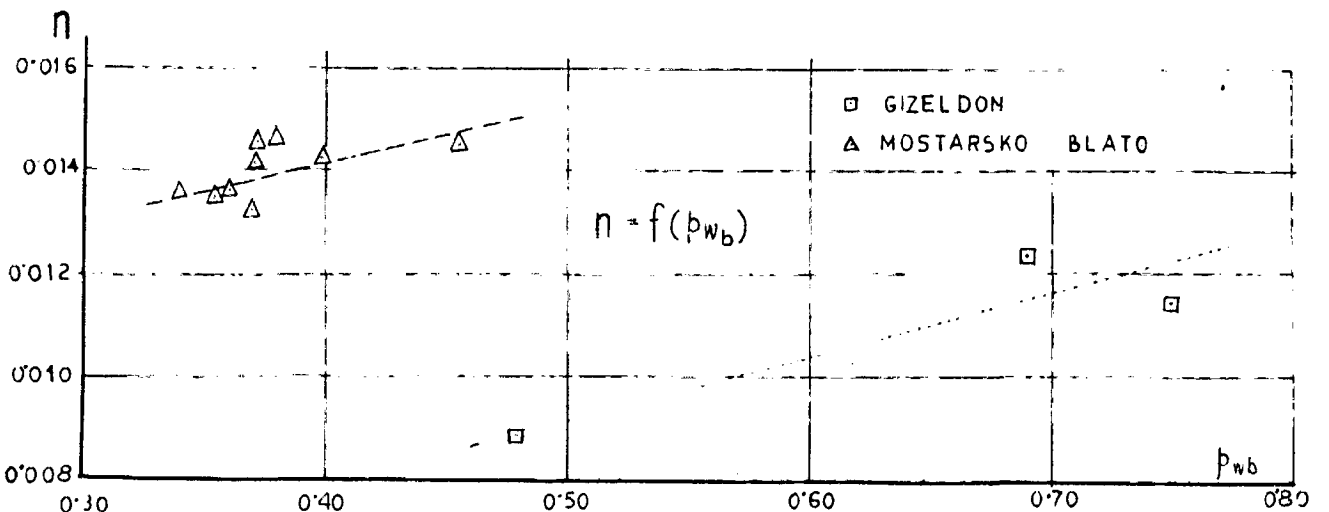


FIG 11 RELATION OF THE RESISTANCE COEFFICIENT  $\eta$  TO THE WATER FACTOR AT THE BOTTOM

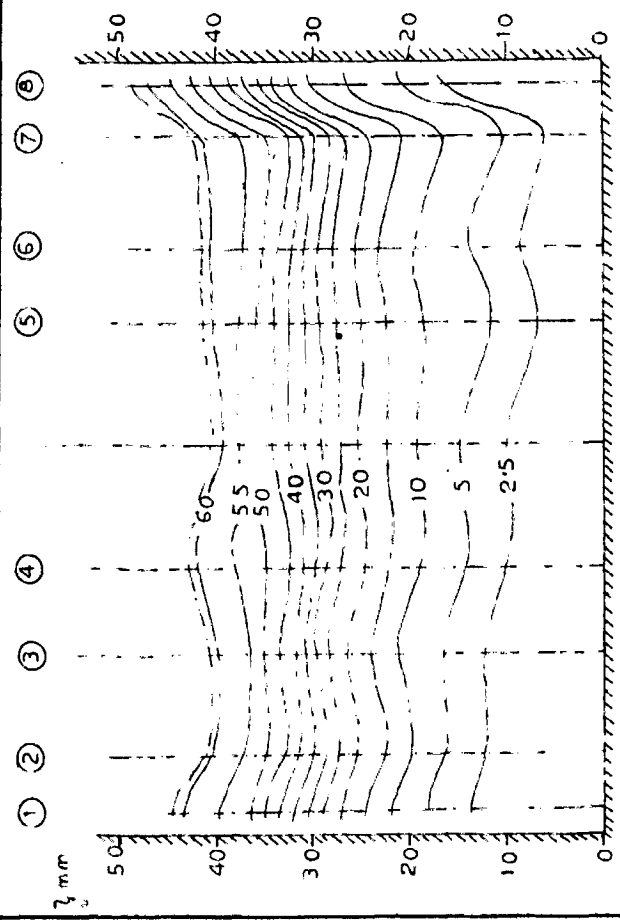


FIG. 12 DISTRIBUTION OF AIR CONCENTRATION IN A CROSS SECTION OF THE FLUME (SLOPE 14) (AIR PERCENTAGES MARKED)

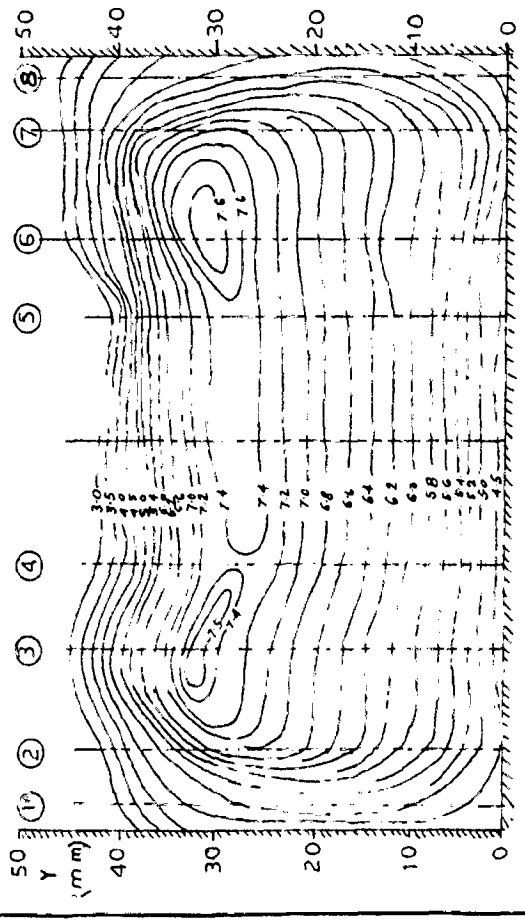


FIG. 13 ISOVELS IN A FLUME CROSS SECTION (SLOPE 14)

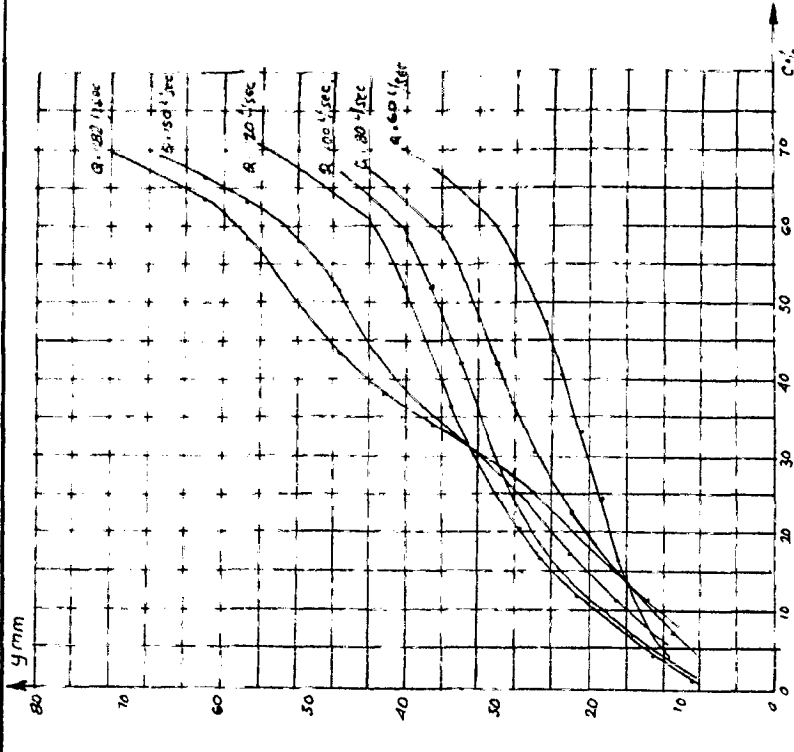


FIG. 14 AIR CONCENTRATION CURVES

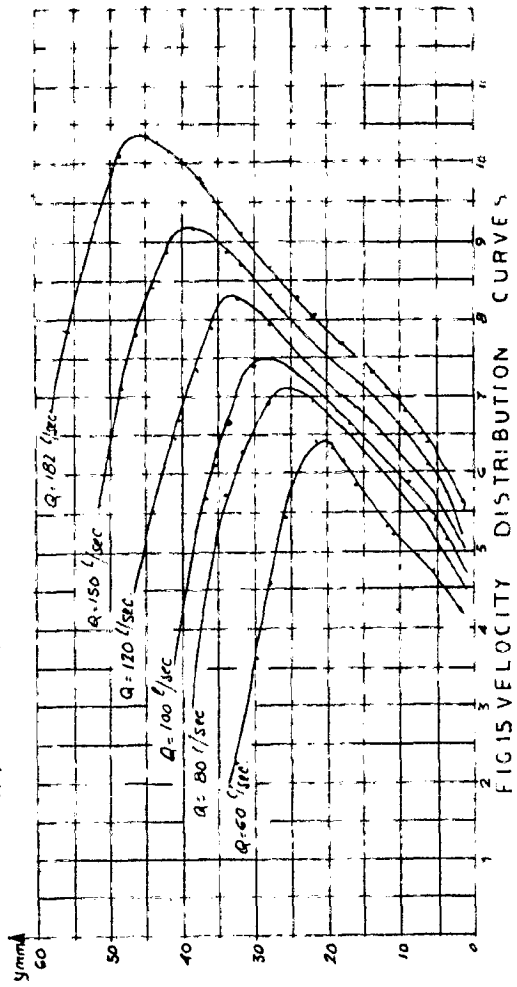


FIG. 15 VELOCITY DISTRIBUTION CURVES

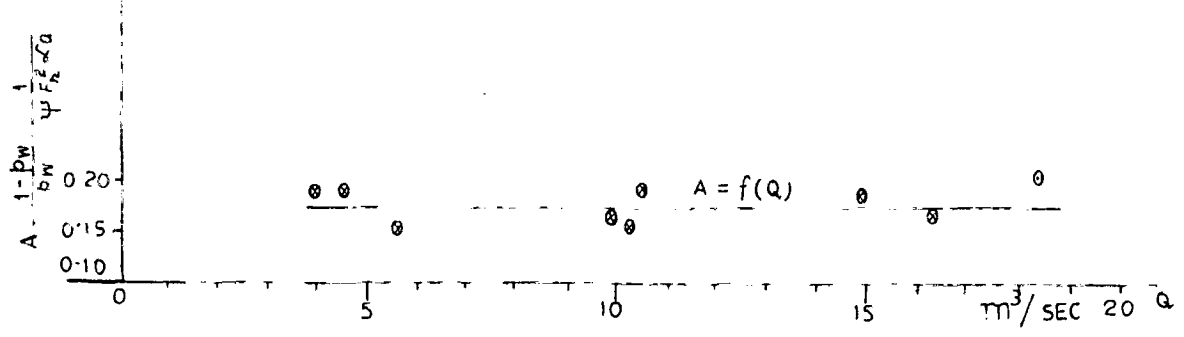


FIG. 6 PLOT OF A VS. Q FROM EXPERIMENTAL DATA OF MOSTARSKO BLATO CHUTE

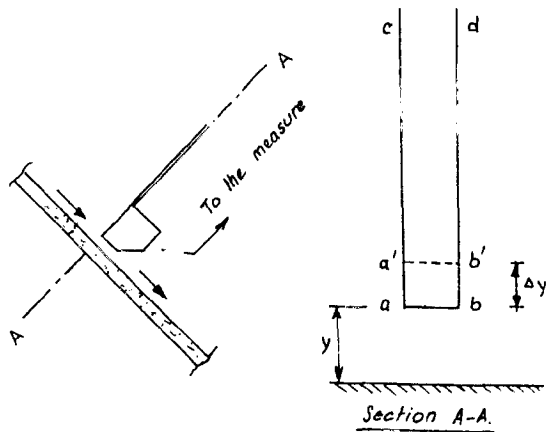


FIG. 17 OPEN SAMPLER SCHEME

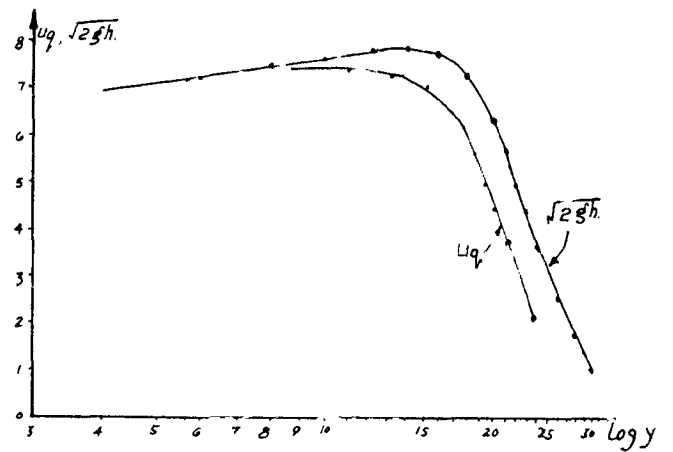


FIG. 18 CURVES  $(u_q, \log y)$  AND  $(\sqrt{2gh}, \log y)$  IN THE SECTION 7.70 M DISTANT FROM THE INLET WITH  $Q=30$  LITERS / SEC

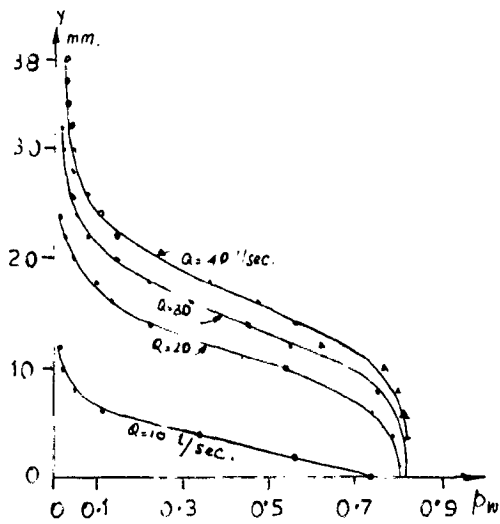


FIG. 19 CURVES  $p_w$  IN AXIS OF THE SECTION 7.70 M DISTANT FROM INLET.

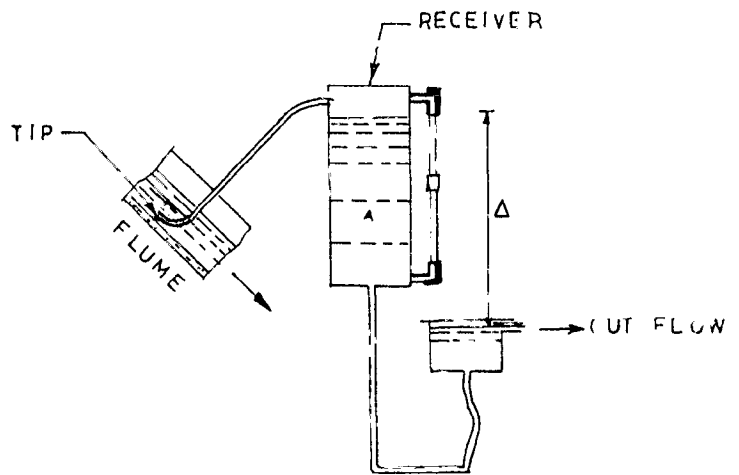


FIG. 20 CLOSED SAMPLER SCHEME

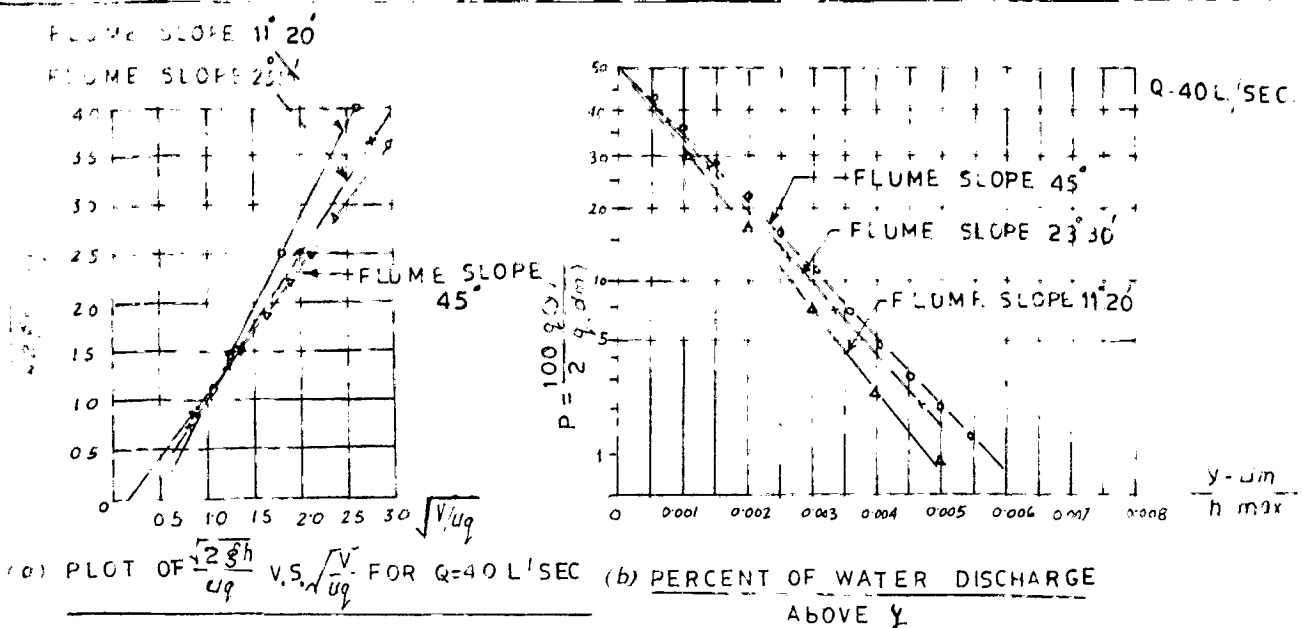


FIG. 21

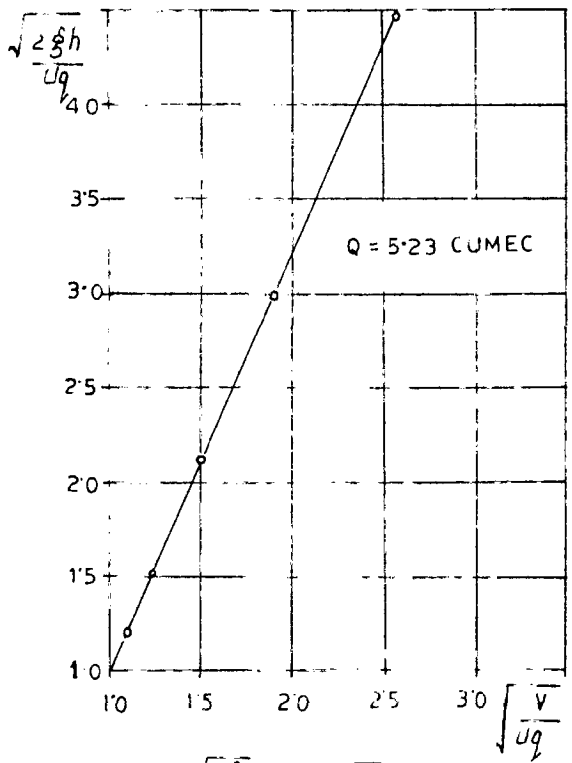


FIG 22 PLOT OF  $\frac{\sqrt{2gh}}{uq}$  V.S.  $\sqrt{\frac{V}{uq}}$  GIZELDON CHUTE

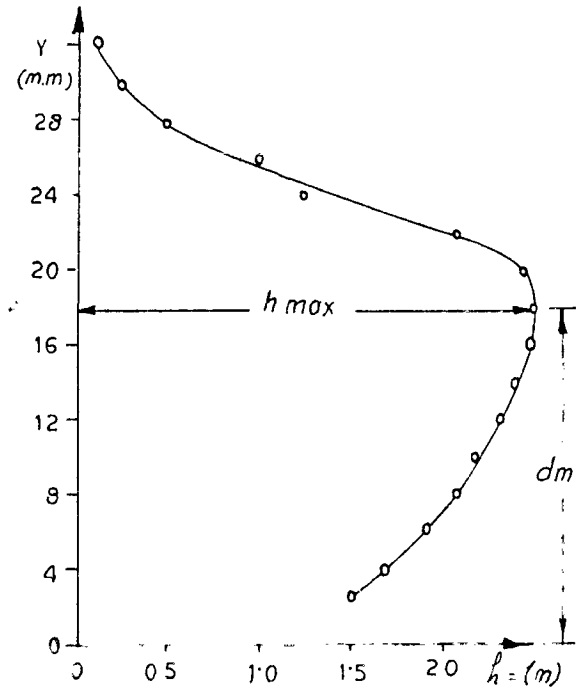
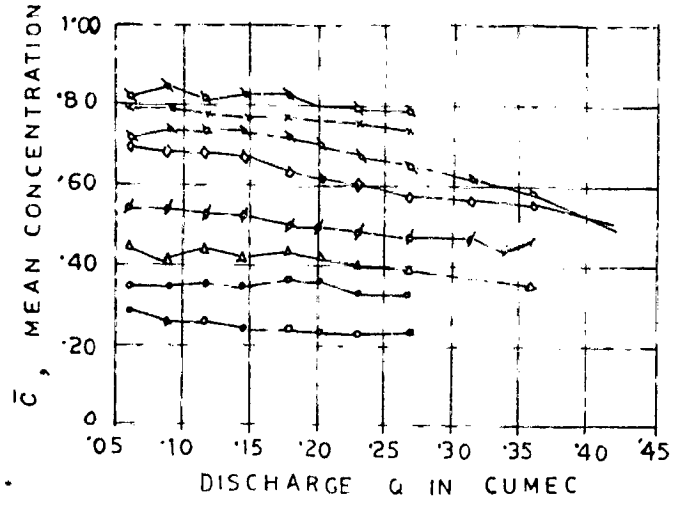


FIG. 23 EXPERIMENTAL CURVE  $h$  vs  $y$



SYMBOL	SLOPE	DEGREE
o	---	7.5
□	---	15.0
△	---	22.5
∩	---	30.0
+	---	37.5
x	---	45.0
*	---	60.0
∧	---	75.0

FIG. 24 AIR CONCENTRATIONS AS FUNCTION OF SLOPE AND DISCHARGE

10/11/55  
UNIVERSITY OF ROORKEE

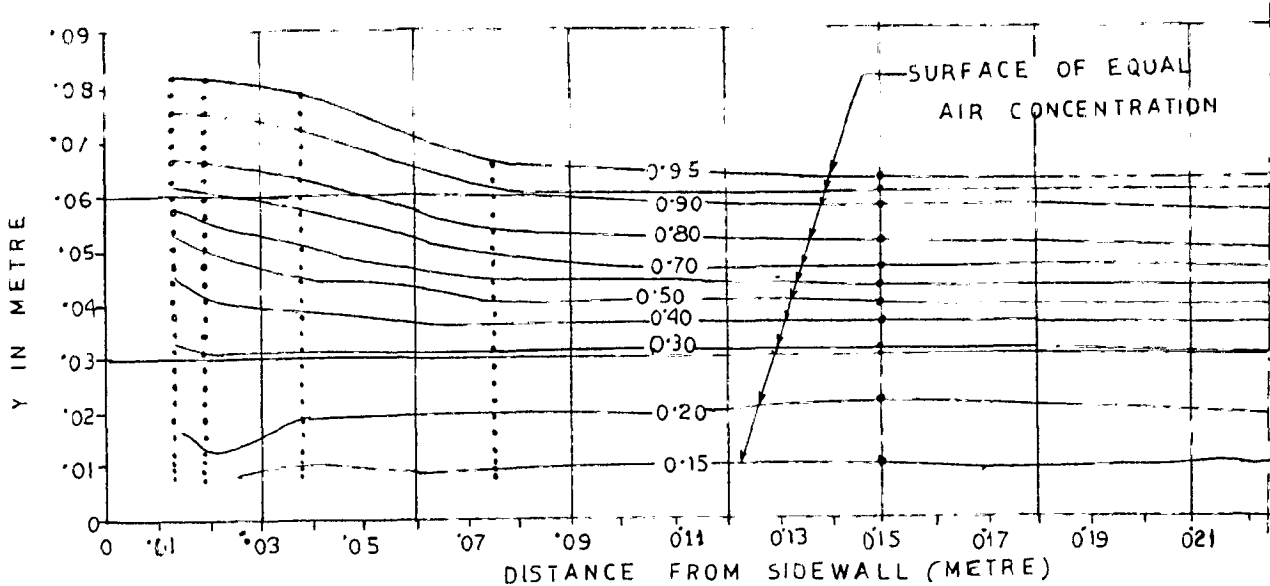


FIG 25 AIR CONCENTRATION DISTRIBUTION ACROSS SECTION OF FULLY AERATED FLOW.

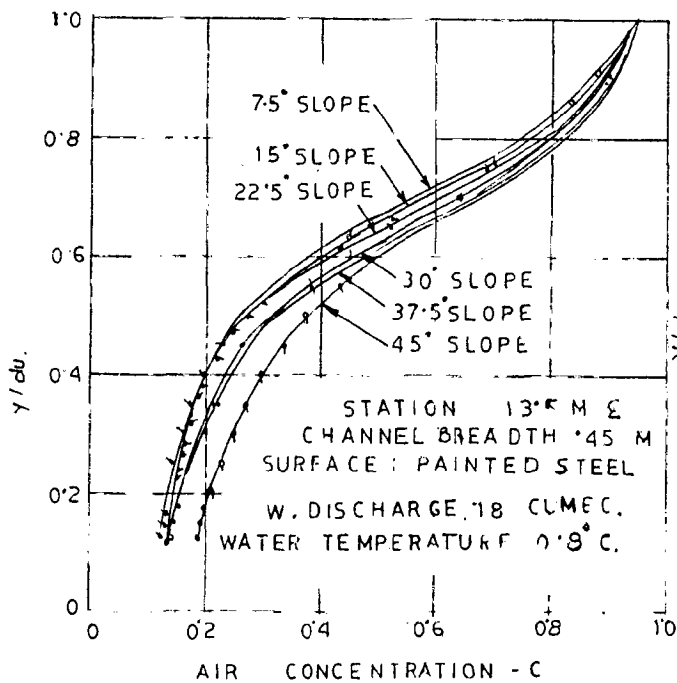


FIG 26 MEASURED AIR CONCENTRATION VALUES IN FULLY AERATED FLOW AT VARIOUS ANGLES WITH CONSTANT DISCHARGE

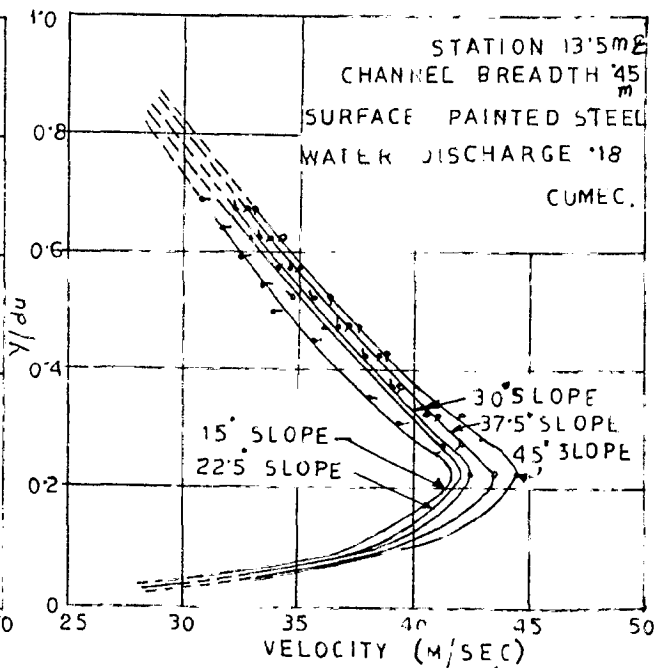


FIG 27. VELOCITY DISTRIBUTION CURVES AT VARIOUS SLOPES FOR CONSTANT DISCHARGE



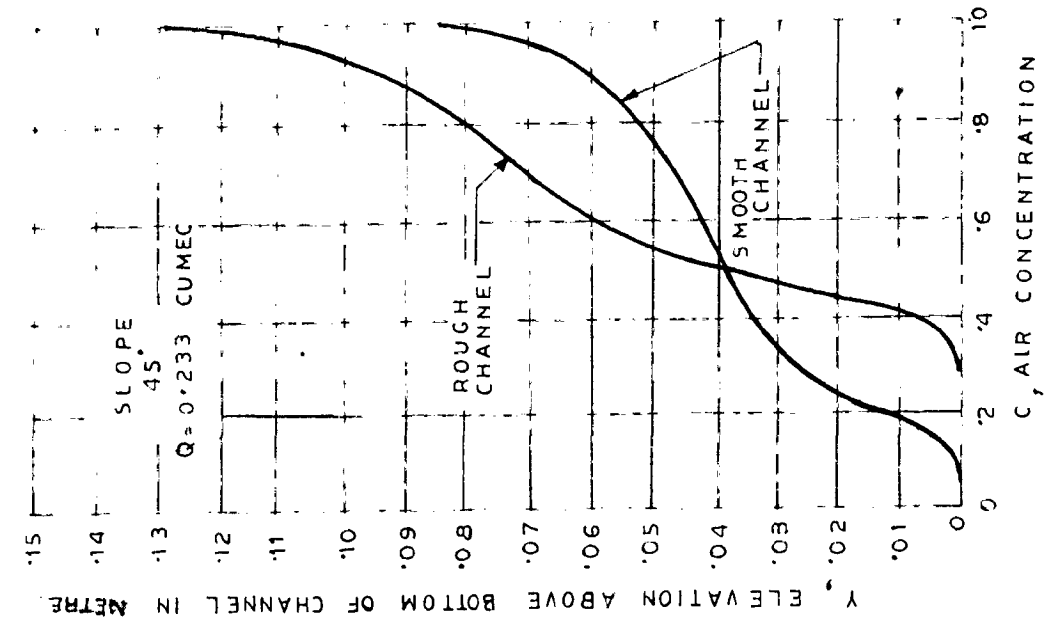


FIG 29 TYPICAL AIR CONCENTRATION PROFILES

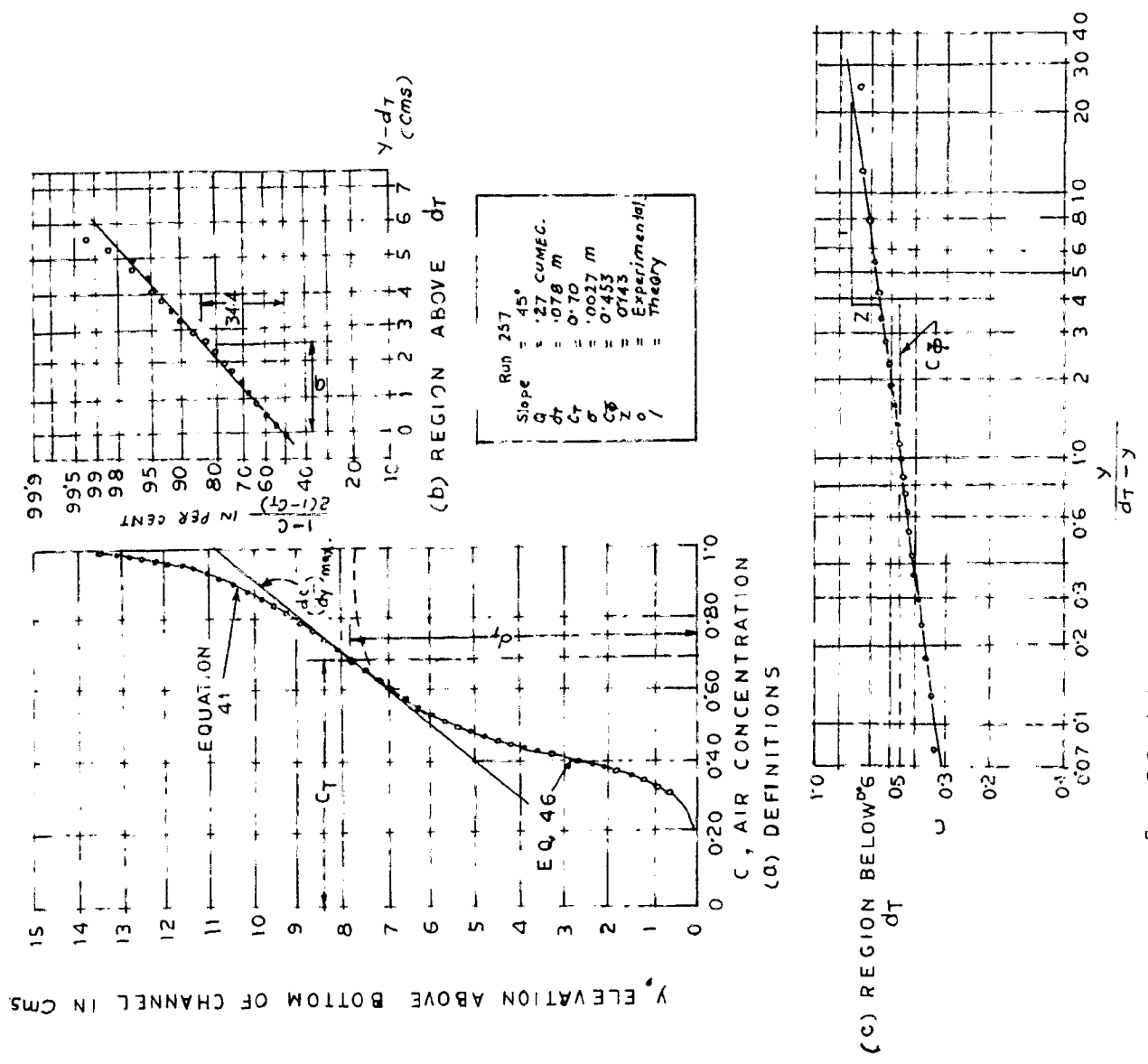


FIG 28 AIR CONCENTRATION DISTRIBUTION PARAMETERS

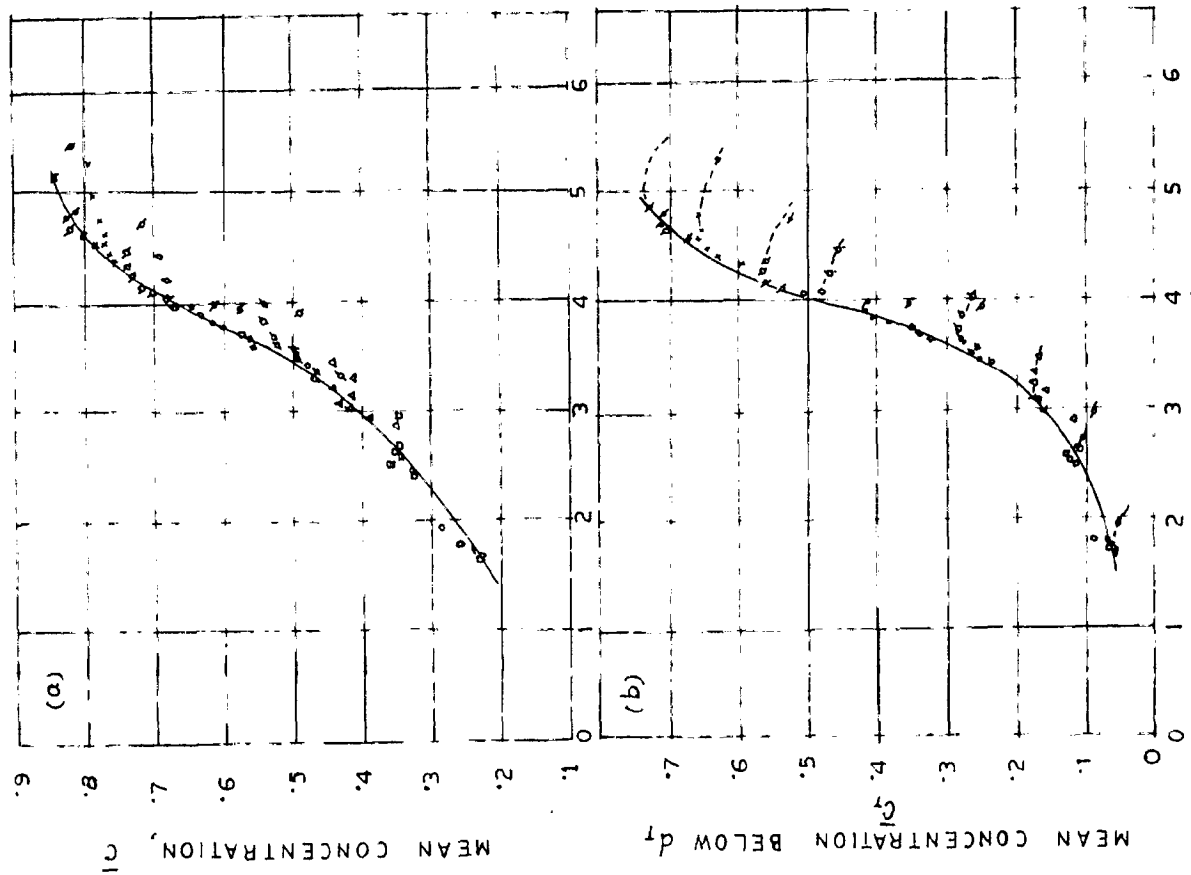


FIG 30 MEAN CONCENTRATIONS AS FUNCTION OF  $v_*/d_1^{2/3}$

LEGEND	
SYMBOL	SLOPE DEG.
o	7.5
□	15
△	22.5
⊙	30
◇	37.5
⊕	45
x	60
⊗	75

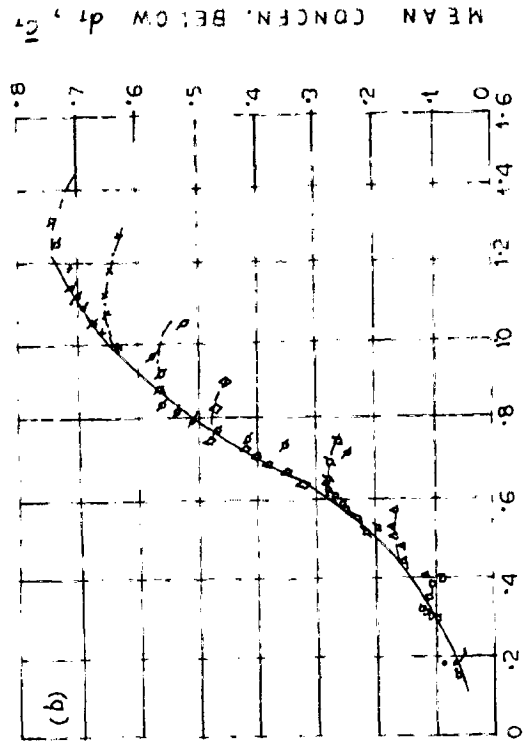
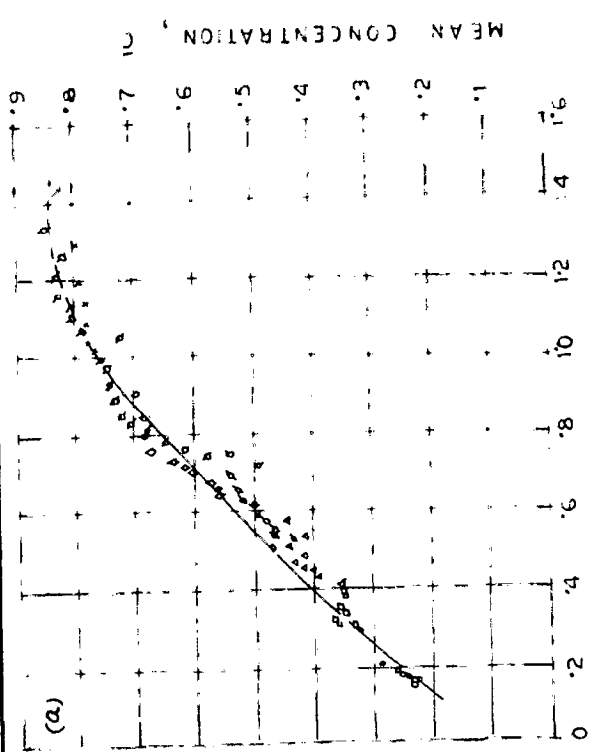


FIG 31 MEAN CONCENTRATIONS AS FUNCTION OF  $s/q^{1/5}$

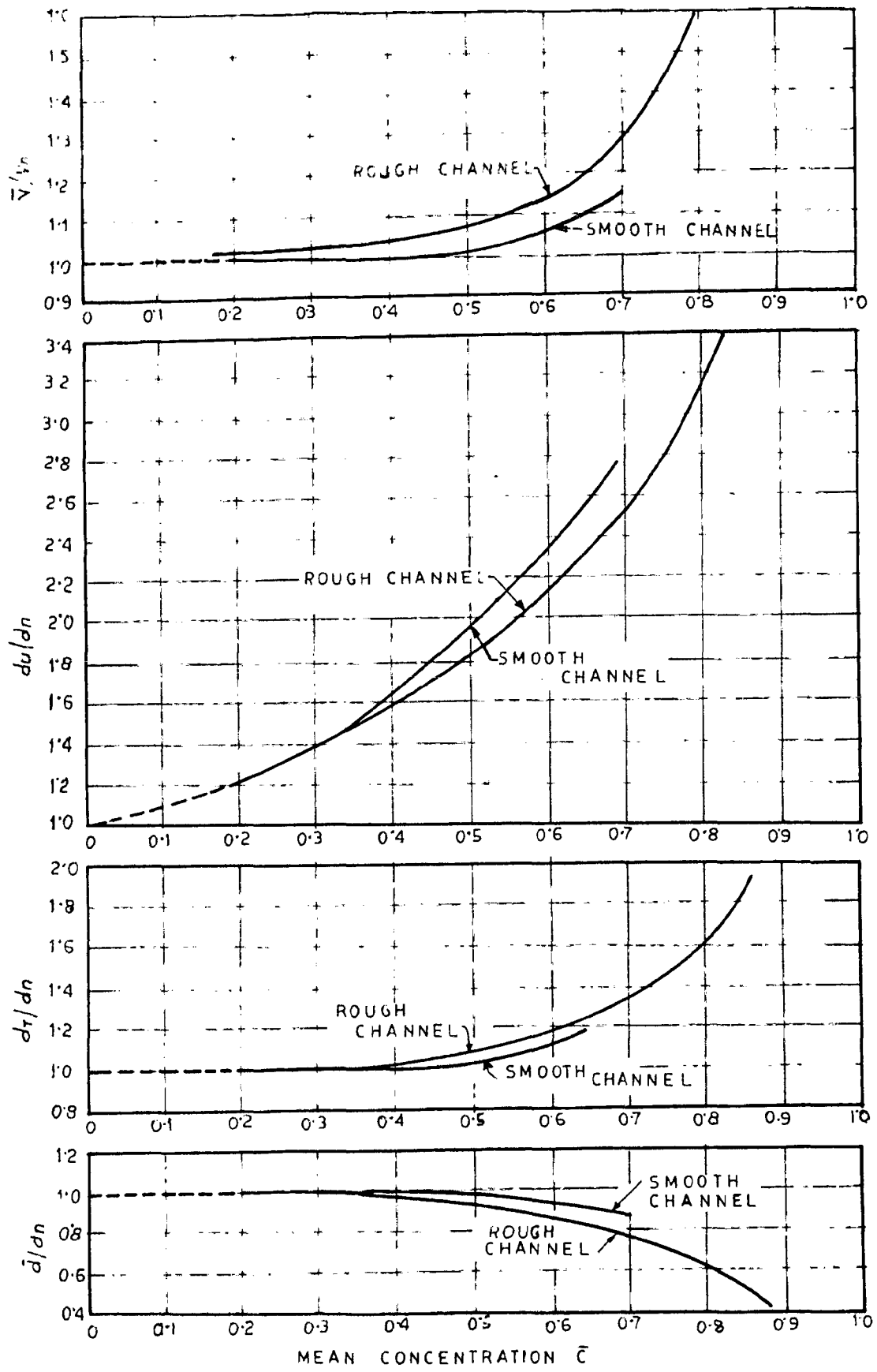


FIG. 32 INFLUENCE OF ENTRAINED AIR ON DEPTHS AND VELOCITY FOR SMOOTH AND ROUGH CHANNELS.

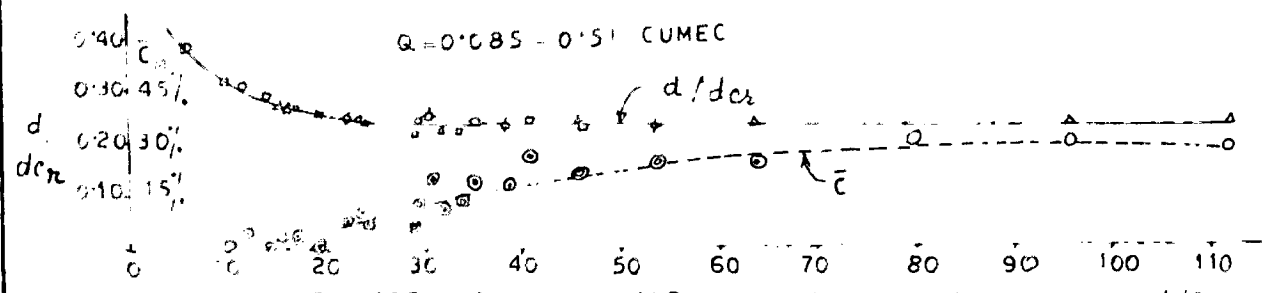


FIG 33 PLOT OF WATER PROFILES AND MEAN AIR ENTRAINMENT (SMOOTH CHANNEL)

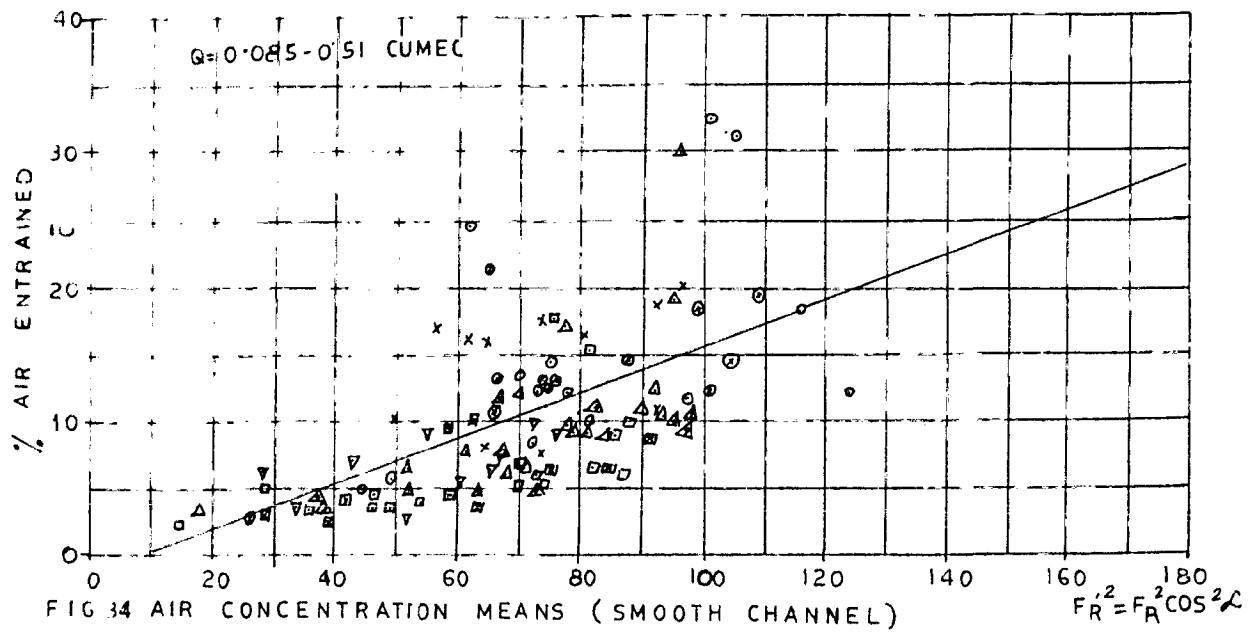


FIG 34 AIR CONCENTRATION MEANS (SMOOTH CHANNEL)

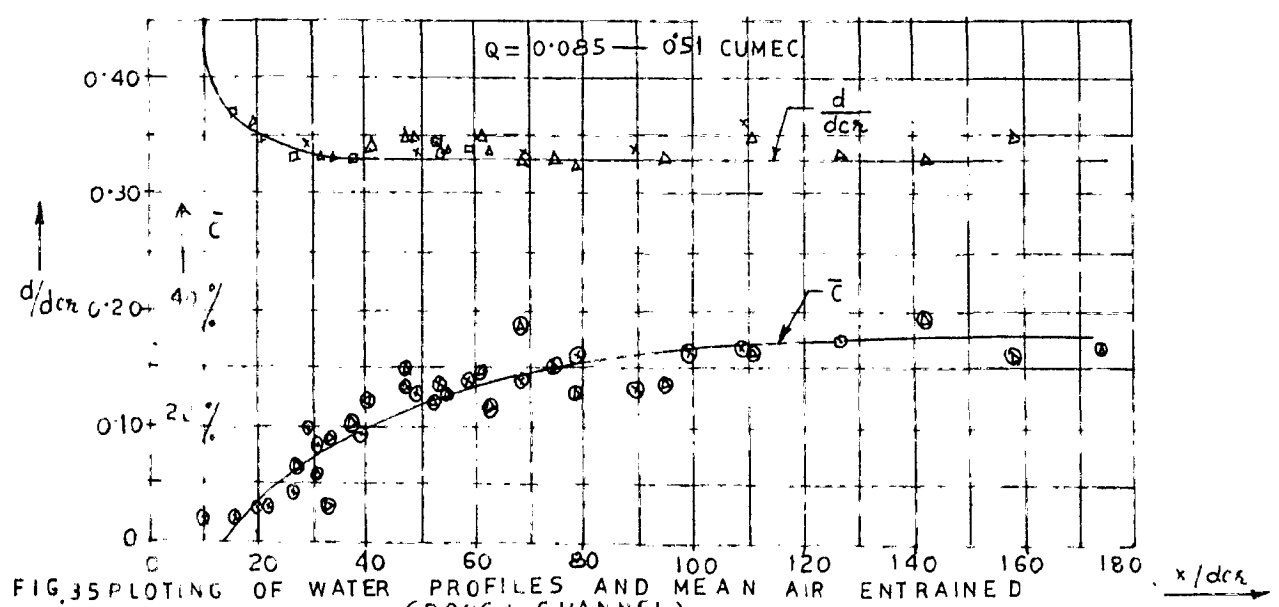


FIG 35 PLOTTING OF WATER PROFILES AND MEAN AIR ENTRAINED (ROUGH CHANNEL)

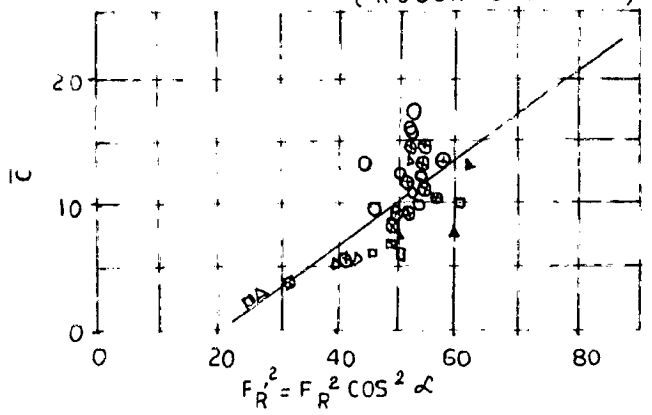


FIG 36 AIR CONCENTRATION MEANS (ROUGH CHANNEL) Q = 0.085 - 0.51 CUMEC.

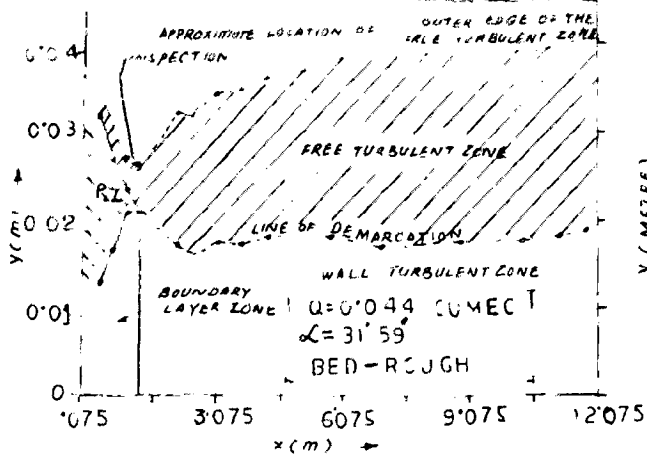


FIG. 37. DEVELOPMENT OF DIFFERENT ZONES IN AERATED FLOW.

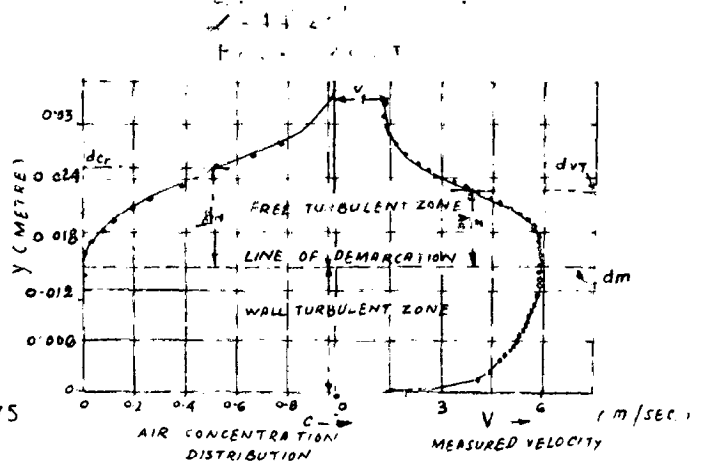


FIG. 38. ZONES IN FULLY AERATED FLOW

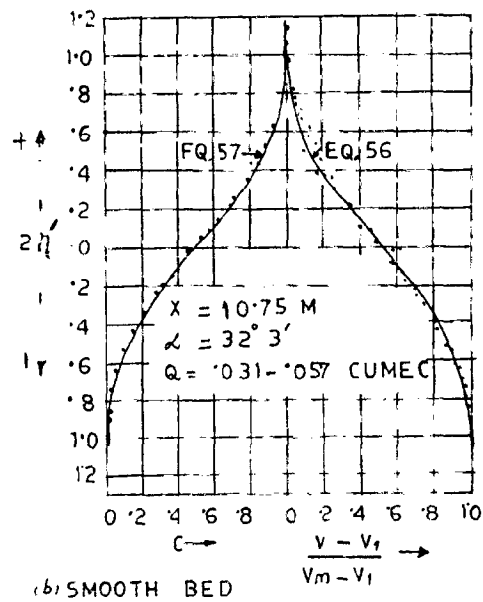
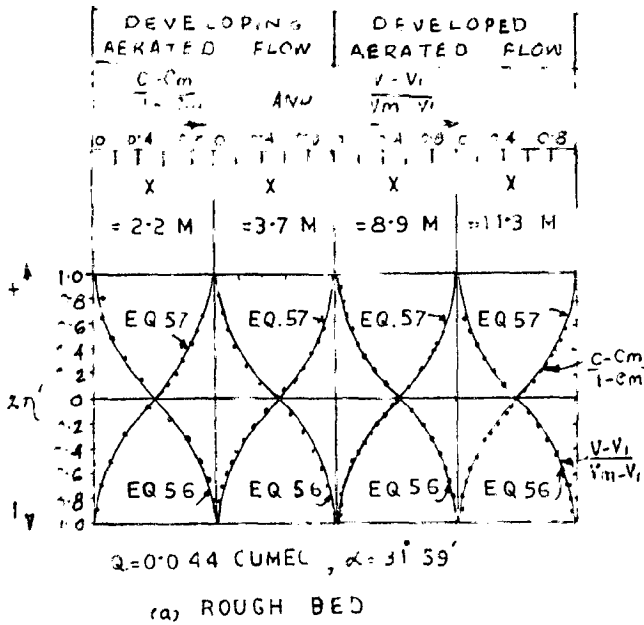


FIG. 39. DISTRIBUTION OF AIR CONCEN. & VELOCITY

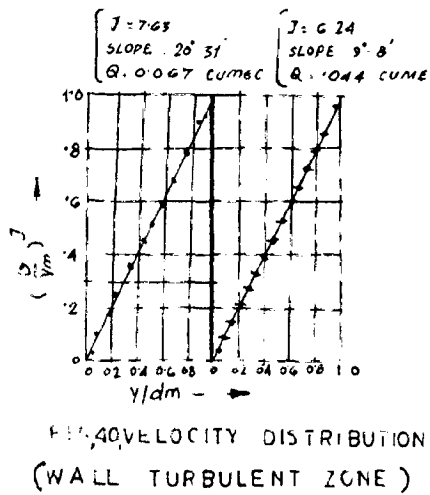


FIG. 40. VELOCITY DISTRIBUTION (WALL TURBULENT ZONE)

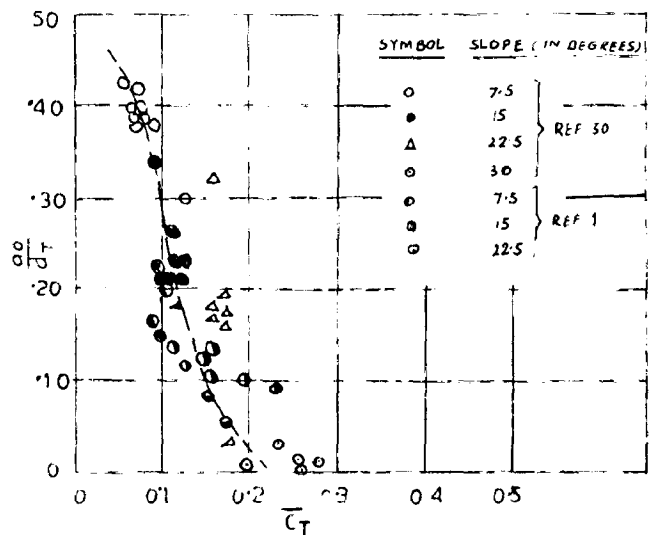


FIG. 41. POSITION OF INNER WALL REGION

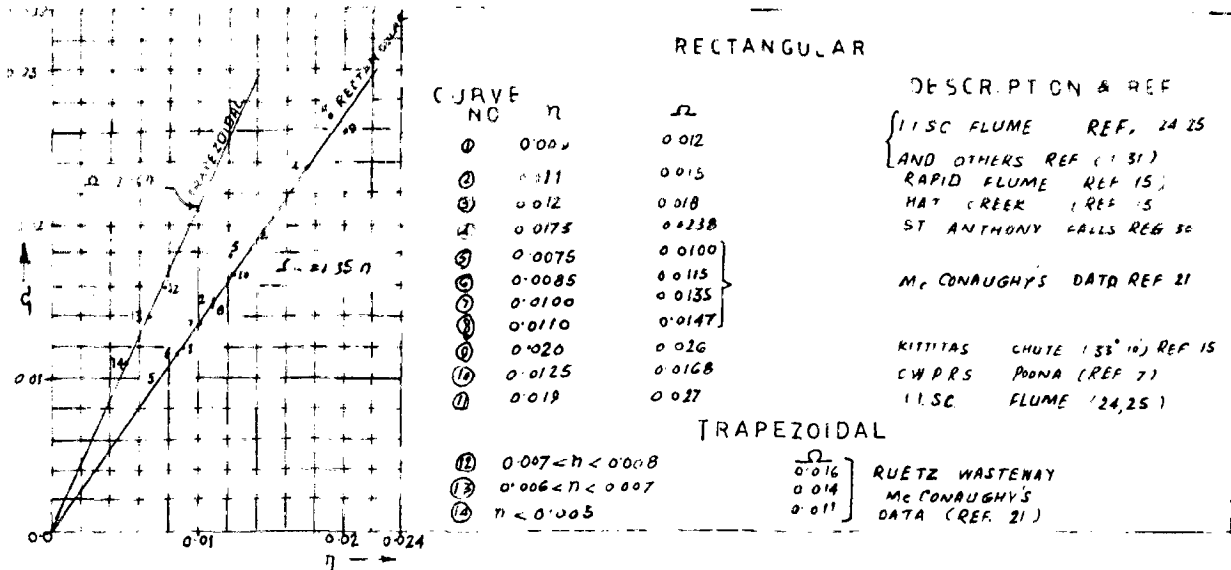


FIG 42 RELATIONSHIP OF n AND zeta

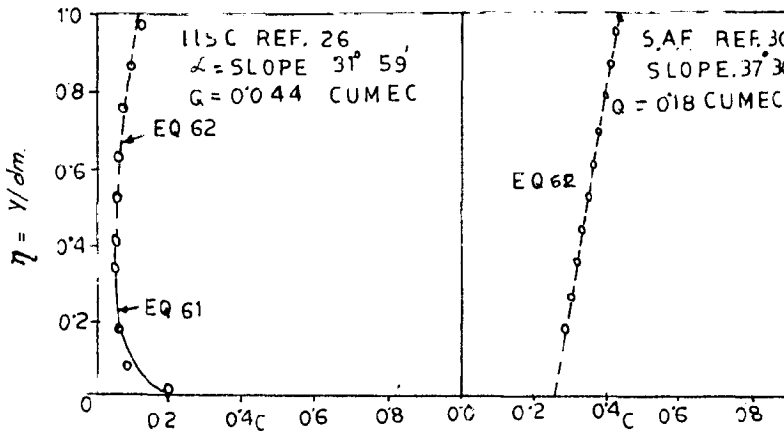


FIG 43 DISTRIBUTION OF AIR CONCENTRATION - WALL TURBULENT ZONE

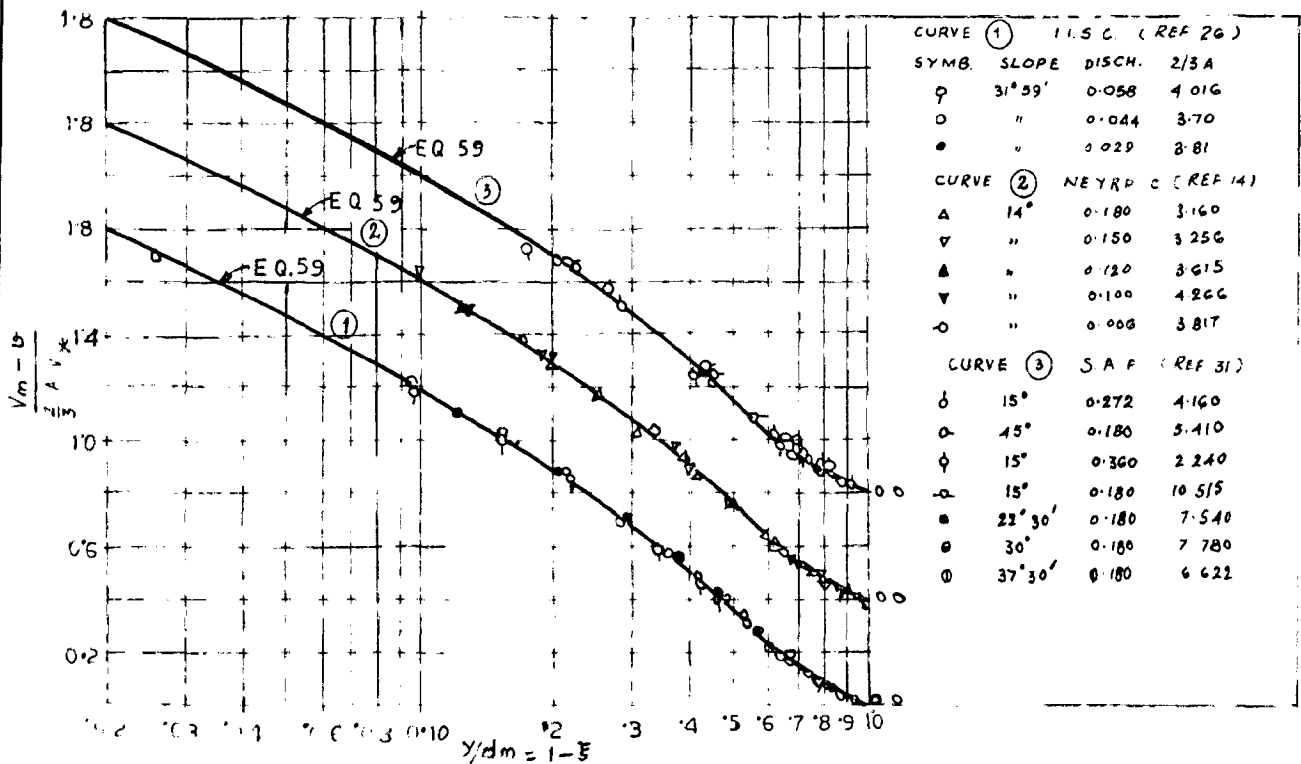


FIG 44 VELOCITY DISTRIBUTION IN WALL TURBULENT ZONE

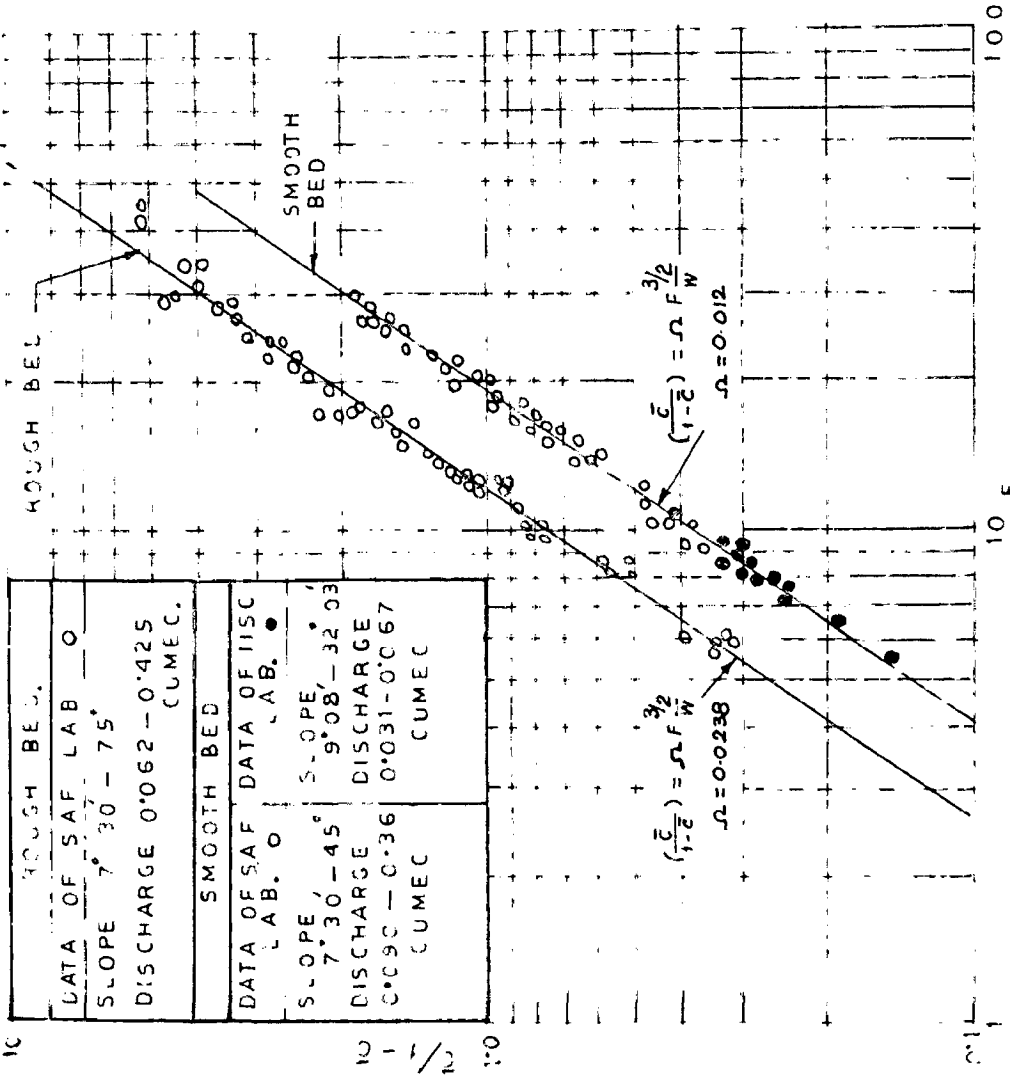


FIG.45 RELATIONSHIP BETWEEN NON AERATED FROUDE NUMBER  $F_w$  AND MEAN AIR CONCENTRATION  $\bar{C}$

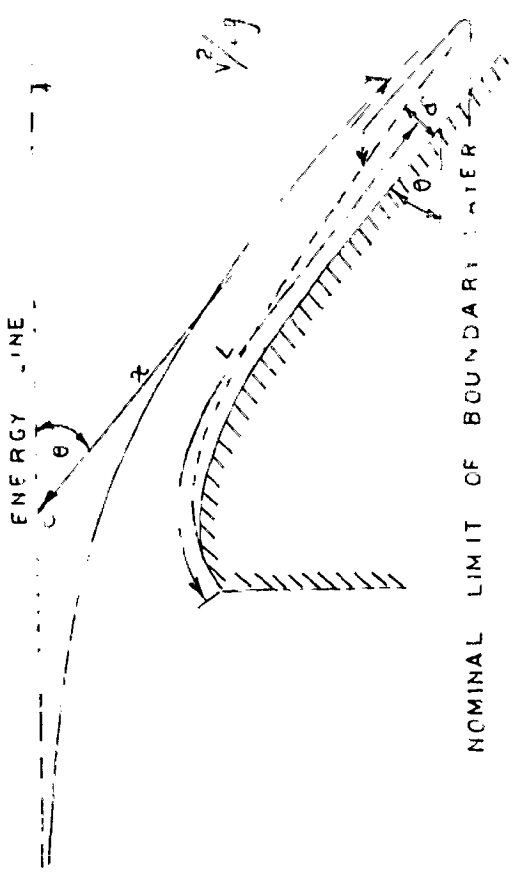


FIG.46 GROWTH OF BOUNDARY LAYER ON SMOOTH SURFACE